

1 **Phylogenomics reveals extensive introgression and a case of mito-nuclear**
2 **discordance in the killifish genus *Kryptolebias***

3 Waldir M. Berbel-Filho^{1,2*}, George Pacheco³, Andrey Tatarenkov⁴, Mateus G. Lira⁶, Carlos
4 Garcia de Leaniz², Carlos M. Rodríguez López⁷, Sergio M. Q. Lima⁶ and Sofia Consuegra²

5 ¹ Department of Biology, University of Oklahoma, Norman, OK, USA (*present address*)

6 ² Department of Biosciences, College of Science, Swansea University, Swansea, UK.

7 ³ Section for Marine Living Resources, National Institute of Aquatic Resources, Technical
8 University of Denmark, Vejlshøvej 39, 8600 Silkeborg, Denmark.

9 ⁴ Department of Ecology and Evolutionary Biology, University of California, Irvine, USA.

10 ⁵ Núcleo de Ecologia Aquática e Pesca da Amazônia, Universidade Federal do Pará, Belém, Brazil.

11 ⁶ Laboratório de Ictiologia Sistemática e Evolutiva, Departamento de Botânica e Zoologia,
12 Universidade Federal do Rio Grande, Natal, Brazil.

13 ⁷ Environmental Epigenetics and Genetics Group, Department of Horticulture, College of
14 Agriculture, Food and Environment, University of Kentucky, Lexington, KY, USA.

15 *Corresponding author: waldirmbf@gmail.com

16 **Highlights**

- 17 • A genomic-based phylogeny is presented for the killifish genus *Kryptolebias*, a genus with
18 a unique diversity of mating systems (e.g., self-fertilization, mixed-mating, outcrossing),
19 covering more species/lineages and genomic loci than previous reconstructions.
- 20 • Nuclear phylogeny and introgression analyses revealed the presence of a previously
21 unknown lineage hidden in a case of mito-nuclear discordance with *K. hermaphroditus*.
- 22 • The new lineage *Kryptolebias* sp. ‘ESP’ possesses high heterozygosity and extensive
23 history of introgression with *K. hermaphroditus*.

24 **Abstract**

25 Introgression is a widespread evolutionary process leading to phylogenetic inconsistencies among
26 distinct parts of the genomes, particularly between mitochondrial and nuclear-based phylogenetic
27 reconstructions (e.g., mito-nuclear discordances). Here, we used mtDNA and genome-wide
28 nuclear sites to provide the first phylogenomic-based hypothesis on the evolutionary relationships
29 within the killifish genus *Kryptolebias*. In addition, we tested for evidence of past introgression in
30 the genus given the multiple reports of undergoing hybridization between its members. Our
31 mtDNA phylogeny generally agreed with the relationships previously proposed for the genus.
32 However, our reconstruction based on nuclear DNA revealed an unknown lineage - *Kryptolebias*
33 sp. 'ESP' – as the sister group of the self-fertilizing mangrove killifishes, *K. marmoratus* and *K.*
34 *hermaphroditus*. All individuals sequenced of *Kryptolebias* sp. 'ESP' had the same mtDNA
35 haplotype commonly observed in *K. hermaphroditus*, demonstrating a clear case of mito-nuclear
36 discordance. Our analysis further confirmed extensive history of introgression between
37 *Kryptolebias* sp. 'ESP' and *K. hermaphroditus*. Population genomics analyses indicate no current
38 gene flow between the two lineages, despite their current sympatry and history of introgression.
39 We also confirmed introgression between other species pairs in the genus that have been recently
40 reported to form hybrid zones. Overall, our study provides a phylogenomic reconstruction
41 covering most of the *Kryptolebias* species, reveals a new lineage hidden in a case of mito-nuclear
42 discordance, and provides evidence of multiple events of ancestral introgression in the genus.
43 These findings underscore the importance of investigating different genomic information in a
44 phylogenetic framework, particularly in taxa where introgression is common as in the sexually
45 diverse mangrove killifishes.

- 46 **Keywords:** Hermaphroditism; Mating systems; Mangrove; Mangrove rivulus, Self-fertilization;
- 47 Rivulidae.

48 **1. Introduction**

49 Estimating the evolutionary relationships among species is a crucial goal of evolutionary
50 biology. With the unprecedented availability of large numbers of loci brought by the genomics
51 era, it has become increasingly clear that organisms generally have a more complex evolutionary
52 history than previously acknowledged, with biological processes such as recombination,
53 incomplete lineage sorting, introgression, and genome rearrangements (Mallet et al., 2016;
54 Nakhleh, 2013) contributing to different phylogenetic signals among topologies generated from
55 different sets of data for the same group of organisms (Bravo et al., 2019).

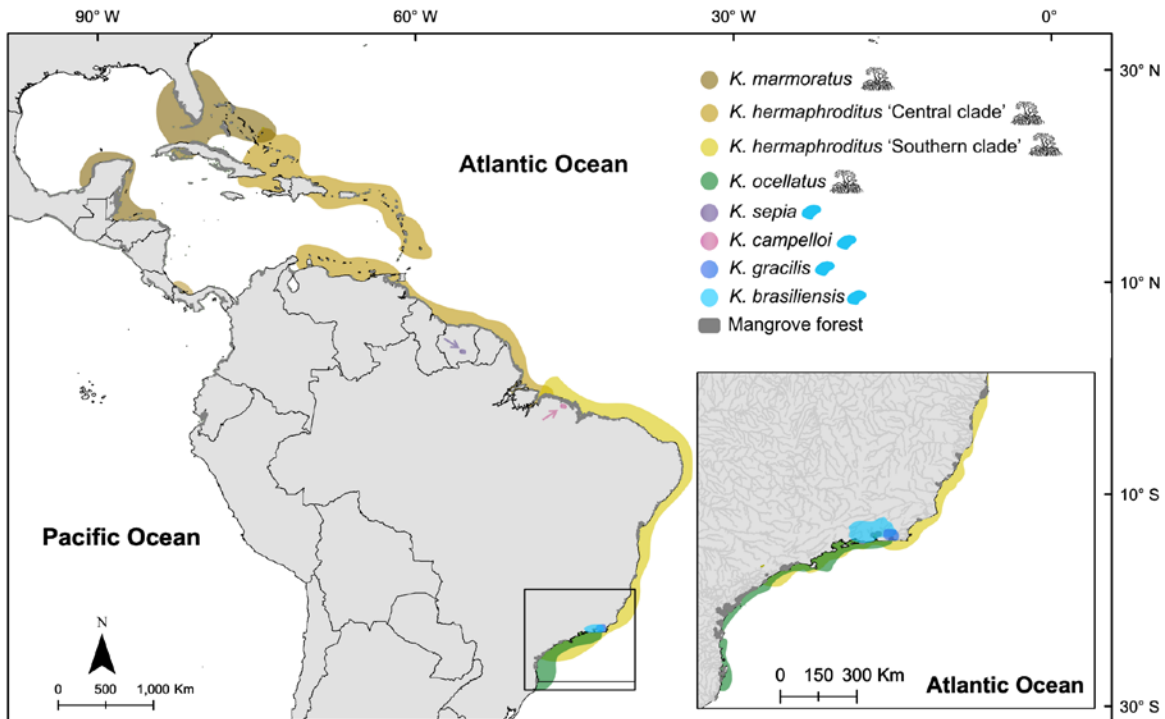
56 Although phylogenetic incongruence may have appeared as a problem at first (Jeffroy et
57 al., 2006; Maddison, 1997), evolutionary biologists now embrace heterogeneity of phylogenetic
58 signals (Bravo et al., 2019; Hahn and Nakhleh, 2016), recognizing that phylogenetic
59 incongruences offer a unique opportunity to investigate the biological phenomena underlying
60 discordance. Among these, reticulate evolution through introgression is today commonly accepted
61 as a widespread evolutionary process contributing to phylogenetic discordance (Bravo et al., 2019;
62 Mallet, 2005; Nakhleh, 2013; Taylor and Larson, 2019). A striking example of how introgression
63 can affect phylogenetic congruence is mito-nuclear discordance, which arises when phylogenetic
64 reconstructions based on mitochondrial or nuclear loci for the same group of organisms
65 substantially differ in their topologies (Bonnet et al., 2017). Although other biological factors (e.g.,
66 incomplete lineage sorting, selection on mtDNA, sex-biased dispersal) are also known to generate
67 mito-nuclear discordances, introgression is commonly pointed out as a major source of mito-
68 nuclear phylogenetic incongruences (Toews and Brelsford, 2012).

69 Differences in mating systems (i.e., defined as the proportion of selfing versus outcrossing
70 in organisms with hermaphrodites (Barrett, 2014)) are expected to influence the extent and

71 direction of hybridization (Pickup et al., 2019) and in the long-term the degree of introgression.
72 For instance, prior selfing (i.e., eggs are self-fertilized before the window for outcrossing) is
73 expected to provide a strong barrier for hybridization given the limited reproductive opportunity
74 for outcrossing (Brys et al., 2016). The variety of mating systems (e.g., predominantly-selfing,
75 mixed-mating, obligately outcrossing) found in the killifish genus *Kryptolebias* provides an ideal
76 opportunity to investigate: i) how different mating systems may affect the extent of hybridization
77 (Berbel-Filho et al., 2021); and ii) the role that introgression between lineages with different
78 mating systems may have on phylogenetic congruence between mitochondrial and nuclear
79 genomes.

80 *Kryptolebias* is a rivulid genus of killifishes (Order Cyprinodontiformes) (Costa, 2011b;
81 Murphy et al., 1999; Thompson et al., 2021), currently composed of seven valid non-seasonal
82 oviparous species (Costa, 2004; Costa, 2011a; Vermeulen and Hrbek, 2005). Previous
83 phylogenetic analyses (based on mtDNA and/or few nuclear genes) proposed two distinct clades
84 within *Kryptolebias*. The ‘freshwater’ clade composed of narrowly distributed freshwater species
85 living in shallow streams and pools in South America: *K. campelloi* (Costa 1990), *K. sepia*
86 Vermeulen & Hrbek 2005, *K. gracilis* Costa 2007, *K. brasiliensis* (Valenciennes 1821). The
87 second clade, known as the ‘mangrove killifishes clade’, is composed of three androdioecious
88 species (i.e., populations consisting of males and hermaphrodites) living on mangrove forests
89 along the tropical and subtropical western Atlantic basin: *K. marmoratus* (Poey 1880), *K.*
90 *hermaphroditus* Costa 2011, and *K. ocellatus* (Hensel 1868)) (Berbel-Filho et al., 2020; Costa et
91 al., 2010; Murphy et al., 1999; Tatarenkov et al., 2017; Tatarenkov et al., 2009; Vermeulen and
92 Hrbek, 2005) (Figure 1). *Kryptolebias marmoratus* and *K. hermaphroditus* are the only two known

93 vertebrate species capable of self-fertilization (selfing) (Awise and Tatarenkov, 2015; Costa et al.,
94 2010; Tatarenkov et al., 2009).



95
96 **Figure 1.** Approximated geographic distribution of known *Kryptolebias* species and lineages.
97 Geographic distributions for the species/lineages were on the literature (Berbel-Filho et al., 2020;
98 Costa, 1990, 2004; Costa, 2007; Costa, 2006, 2016; Lira et al., 2021; Tatarenkov et al., 2017;
99 Vermeulen and Hrbek, 2005) as well as online databases for sampling records (GBIF;
100 www.gbif.org) and museum collections (CRIA - SpeciesLink; <http://splink.cria.org.br/>). Symbols
101 next to species name represent species inhabiting mangrove (mangrove tree) or freshwater (blue
102 spot) habitats.

103 In the selfing mangrove killifish species (*K. marmoratus* and *K. hermaphroditus*), most of
104 the eggs laid externally are already fertilized via selfing (Harrington, 1971; Lomax et al., 2017),

105 leaving a limited window of opportunity for outcrossing either by intra or heterospecific males.
106 Despite this expected limitation, recent studies identified cases of undergoing hybridization
107 involving the selfing *Kryptolebias* species. Tatarenkov et al. (2018) (and later expanded by
108 Tatarenkov et al. (2021)) reported hybridization between highly-selfing lineages of *K. marmoratus*
109 and *K. hermaphroditus* ‘Central clade’ (a lineage closely related to *K. hermaphroditus* present in
110 the southern portions of the Caribbean, Central America, and northern South America, with
111 taxonomic status still under debate (Lira et al., 2021; Tatarenkov et al., 2017)). In Southeast Brazil,
112 two hybrid zones formed by interbreeding between *K. hermaphroditus* (predominantly-selfing,
113 (Berbel-Filho et al., 2019)) and *K. ocellatus* (exclusively outcrossing, (Berbel-Filho et al., 2020))
114 represented the first known case of hybridization between species with different mating systems
115 in vertebrates (Berbel-Filho et al., 2021). These unlikely hybridization cases called for further
116 research on the role of past introgression in the diversification of the genus *Kryptolebias*.

117 Although *K. hermaphroditus* populations are mostly composed of selfing hermaphrodites,
118 outcrossing occasionally happens (Berbel-Filho et al., 2019), most likely involving rare males and
119 hermaphrodites (Furness et al., 2015). Despite historical sampling, particularly in Southeast Brazil
120 (Costa, 2011a), males of *K. hermaphroditus* were only reported recently (Berbel-Filho et al., 2016;
121 Costa, 2016). Costa (2016) reported a relatively high frequency of *K. hermaphroditus* males (e.g.,
122 three out of 20 individuals) in a single population in the Brazilian state of Espírito Santo. In
123 rivulids, the male color pattern is the most conspicuous character to diagnose species (Costa 2003).
124 This is particularly true for the mangrove killifish clade, in which hermaphrodites are remarkably
125 similar morphologically (Costa, 2011a, 2016). Therefore, Costa (2016) argued that the color
126 patterns observed (in two different ‘morphs’) in *K. hermaphroditus* males from this Espírito Santo
127 and other locality in the Rio de Janeiro state represented an important diagnostic trait to the

128 morphological identification of species in the group (Costa, 2009). However, the pattern of
129 coloration of the *K. hermaphroditus* males reported by Costa (2016) differed substantially from
130 the male color reported for *K. hermaphroditus* in Berbel-Filho et al. (2016) as well as other males
131 reported for the species (Supplementary Figure S1; Amorim et al., 2022). Particularly the ‘dark
132 morph’ (Costa 2016), which exhibited a dark body flank with broad black margin along the whole
133 caudal fin, while the ‘light morph’ and the other *K. hermaphroditus* males found in other
134 populations exhibited an orange pattern of pigmentation along its body and often had faded black
135 margins in the caudal fin (Supplementary Figure S1). The relatively high frequency of males, the
136 presence of male two color morphs and the disparity in their coloration, together with the multiple
137 evidence for hybridization in mangrove killifishes prompted further research on the identity and
138 evolutionary history of the unusual Espírito Santo locality in Brazil.

139 The reports of undergoing hybridization (Berbel-Filho et al., 2021; Tatarenkov et al., 2018,
140 2021), as well as the recent advances in the knowledge of natural history and distribution of
141 *Kryptolebias* species (Berbel-Filho et al., 2019; Berbel-Filho et al., 2020; Costa, 2016; Guimarães-
142 Costa et al., 2017; Lira et al., 2021; Sarmiento-Soares et al., 2014; Tatarenkov et al., 2017) highlight
143 the need of an updated hypothesis regarding the evolutionary relationships within the genus
144 *Kryptolebias*. Using a phylogenomic approach together with a higher number of loci and
145 taxonomic sampling than previous phylogenetic reconstructions, our study aimed to provide the
146 first phylogenomic-based hypothesis for the species relationships in *Kryptolebias*. In addition, we
147 aimed to investigate the hypothesis that reticulation and past introgression events contributed to
148 the diversification of *Kryptolebias* lineages. We reveal a previously unknown lineage/species with
149 strong evidence of ancestral introgression hidden in a case of mito-nuclear discordance. Our

150 findings highlight how the use of a phylogenomic approach can shed light on the phylogenetic
151 history of groups with common history of interspecific hybridization and challenging taxonomy.

152 **2. Material and Methods**

153 **2.1. Mitochondrial DNA dataset**

154 We generated a cytochrome oxidase 1 (*cox1*) dataset of 423 sequences from 50 sampling
155 localities and five out of the seven species (with exception of *K. sepia* and *K. campelloi*) formally
156 described as *Kryptolebias* species. Given the high nuclear divergence found in the Espírito Santo
157 locality in the ‘Southern clade’ with nuclear data (see results below), we incorporated sequences
158 for 18 individuals from this population generated here. Three additional *cox1* sequences for species
159 in the ‘freshwater’ clade, namely *K. gracilis* and *K. brasiliensis* were also generated here, while
160 the remaining samples were extracted from previously published data. The samples processed for
161 this study followed primers and PCR protocols described in Tatarenkov et al. (2017). Both forward
162 and reverse DNA strands were sequenced and assembled using Geneious v. 9.1.8
163 (www.geneious.com). A detailed list of samples used in the mtDNA analyses is presented in
164 Supplementary Table S1.

165 2.2. Mitochondrial Phylogeny and haplotype network

166 Our dataset containing 423 *Kryptolebias* individuals was reduced to unique 49 *cox1*
167 haplotypes of 591bp. A *cox1* sequence from *Atlantirivulus santensis* (Köhler 1906) (GenBank
168 accession number GU701924.1) was used as an outgroup for the phylogenetic reconstructions. We
169 identified the best partition scheme and substitution models using ModelFinder in IQ-Tree2 v.
170 2.1.0 (Kalyaanamoorthy et al., 2017; Minh et al., 2020). We used the suggested partition scheme
171 to infer a maximum likelihood reconstruction and inferred uncertainty with 1000 standard non-
172 parametric bootstrap iterations. Given the evidence of mito-nuclear discordance within the selfing
173 mangrove killifishes clade (see results below), we isolated the 27 haplotypes within this clade and
174 used POPART v. 1.7 (<https://popart.otago.ac.nz/>) to generate a TCS haplotype network (Clement
175 et al., 2002).

176 2.3. Nuclear DNA dataset

177 We combined newly-generated and previously-published data to generate a nuclear DNA
178 dataset across *Kryptolebias* species. First, we sampled populations of *K. ocellatus* (sensu Costa
179 2011), *K. hermaphroditus* (sensu Costa 2011), *K. brasiliensis* and *K. gracilis* during a field trip in
180 Southeast Brazil between August and September 2017. We collected the fish using hand nets.
181 *Kryptolebias ocellatus* and *K. hermaphroditus* are syntopic in their type-locality (GUA in
182 Supplementary Fig. S3) (Berbel-Filho et al., 2020). Sampling was conducted under license
183 ICMBio/SISBIO 57145-1/2017 and approved by Swansea University Ethics Committee reference
184 SU-Ethics-Student-250717/245.

185 We build a genotype-by-sequencing library (GBS) for a total of 96 fin clips samples. DNA
186 was extracted the using Qiagen DNeasy Blood and Tissue kit (Qiagen, Hilden, Germany)
187 following the manufacturer's protocol. GBS libraries were prepared as described in Kitimu et al.

188 (2015). In brief, extracted DNA was digested using the restriction enzymes EcoRI and HpaII and
189 ligated to sequencing adapters. Those enzymes were selected based on successful sampling of
190 many restriction sites in *K. hermaphroditus* populations (Berbel-Filho et al., 2019). An aliquot of
191 200 ng of genomic DNA were digested using a EcoRI (cutsite: GAATTC) and HpaII (cutsite:
192 CCGG). Digested DNA was ligated to individually barcoded adapters with a HpaII cut site
193 overhang and a common EcoRI Y adapter. Ligation products were individually cleaned to remove
194 excess of adapters using Agencourt AMPure XP purification system (#A63880, Beckman Coulter,
195 Brea, CA, USA) at a v/v ratio of 0.85 following the manufacturer's instructions. A single library
196 was produced by pooling 20 ng of digested DNA from each restriction/ligation product and
197 amplified in eight separate PCR reactions which were pooled after amplification, size-selected
198 (range 200–350 bp) and sequenced in a single lane of an Illumina NextSeq500 sequencer.

199 Out of the original 96 samples included in the library, 61 (36 *K. ocellatus* and 25 *K.*
200 *hermaphroditus*) had been analysed in Berbel-Filho et al. (2021), while the remaining 35 (13 *K.*
201 *gracilis*, 11 *K. brasiliensis* and 11 individuals from the Espírito Santo population) were generated
202 specifically for the present study. We extracted 11 *K. hermaphroditus* and 9 *K. ocellatus* GBS
203 samples from Guaratiba (type-locality for both species) previously published in Berbel-Filho et al.
204 (2021). Furthermore, to expand our taxonomic sampling of *Kryptolebias* species, we incorporated
205 raw whole-genome sequencing data for *K. marmoratus* individuals from Florida, Belize,
206 Honduras, and San Salvador Island obtained by Lins et al. (2018). Additional raw whole-genome
207 sequencing data for localities from Guantanamo Bay in Cuba (from Lins et al. (2018)) and Panama
208 (from Choi et al. (2020)), representing individuals from the 'Central clade' lineage were also
209 included. These samples represent a lineage closely related to *K. hermaphroditus* present in the
210 Greater Antilles, Lesser Antilles, southern Central America, and northern portions of South

211 America (Lira et al., 2021; Tatarenkov et al., 2017). The formal taxonomic status of the ‘Central
212 clade’ lineage (i.e., either as a distinct species or a differentiated lineage of *K. hermaphroditus*) is
213 still under debate (Lira et al., 2021; Tatarenkov et al., 2021; Tatarenkov et al., 2017). To
214 simultaneously highlight its proximity and divergence with *K. hermaphroditus*, we refer to
215 mtDNA and SNPs data from individuals of the ‘Central clade’ as “*K. hermaphroditus* ‘Central
216 clade’” throughout the manuscript. Data from *K. hermaphroditus* individuals from Southeast
217 Brazil is referred as “*K. hermaphroditus* ‘Southern clade’” following the classifications in Lira et
218 al. (2021) and Tatarenkov et al. (2017). Similarly to the mtDNA dataset, we were unable to get
219 hold of samples from the freshwater species *K. sepia* and *K. campelloi*. Those species are only
220 known from very limited geographical distributions in creeks in the Amazon Forest (Costa 1990;
221 Vermeulen and Hrbek, 2005) (Figure 1). No further reports for neither of those species have been
222 found since the sampling reported in the original description (2003 for *K. sepia* in Vermeulen et
223 al., (2006); 1974 for *K. campelloi* in Costa (1990)). We also incorporated raw whole-genome
224 sequencing data for *Nematolebias whitei* (Myers 1942) from Thompson et al., (2022), to be used
225 as an outgroup in the phylogenetic reconstruction based on concatenated nuclear sites.

226 2.3.1. Nuclear DNA data processing

227 We used GBSX v1.3 (Herten et al., 2015) to demultiplex the paired-end reads data from
228 the GBS library allowing for one mismatch in the barcodes (-mb 1), no mismatch in the enzyme
229 cut-site (-me 0) and ensuring that no common sequencing adapter was to be removed (-ca false).
230 We then filtered (-qtrim r; -minlength 25) and merged the GBS reads by individuals using BBmap
231 tools (Bushnell, 2014). All samples (both from GBS and whole-genome sequencing) were mapped
232 to the assembled *Kryptolebias hermaphroditus* reference genome (Choi et al., 2020) using either
233 BWA v0.7.17 (for the phylogenetic reconstruction – Dataset I) or Bowtie 2 v2.3.5 (for analyses

234 within *Kryptolebias* - Datasets II to VIII) using default parameters (Langmead and Salzberg, 2012)
235 and generated filtered and indexed individual BAM files using samtools v 1.10.0 (Li et al., 2009).
236 The different aligners were used due to their different mapping algorithms. While Bowtie2 tends
237 to have faster throughput, it does that at the expense of mapping a lower number of reads when
238 compared to BWA (Hatem et al., 2013). This can dramatically decrease the number of sites shared
239 across samples, especially when a distantly related sample is incorporated in the dataset (i.e., an
240 outgroup). For this reason, we used BWA v.07.17 (Li and Durbin, 2009) as the aligner in the
241 dataset incorporating the *N. whitei* outgroup sample (Dataset I), while the remaining datasets
242 including only *Kryptolebias* samples (Datasets II to VIII) had Bowtie2 v2.3.5 (Langmead and
243 Salzberg, 2012) as an aligner. For the whole-genome samples extracted from the literature, we
244 removed sequencing adapters using AdapterRemoval v. 2.2.2 (Schubert et al., 2016), mapped
245 samples to *K. hermaphroditus* genome using either BWA v0.7.17 (for phylogenetic reconstruction
246 – Dataset I) or Bowtie 2 v2.3.5 (for analysis within *Kryptolebias* – Datasets II to VIII) and filtered
247 and indexed individual BAM files using samtools v1.10.0 within a pipeline in Paleomix v1.3.2
248 (Schubert et al., 2014). We limited our dataset to samples with $\geq 500k$ reads. These resulted in a
249 dataset of 48 (out of 61) *Kryptolebias* samples. A detailed list of the samples and sampling
250 localities is provided in Supplementary Table S2.

251 2.3.2. Variant calling

252 For all datasets analysed (details provided in Table S4), we inferred genotypes using
253 ANGSD v0.9.32 (Korneliussen et al., 2014). Due to the methylation sensitivity of HpaII, we
254 constrained our variant calling to a maximum of 5% of missing data per loci across all individuals.
255 We used ANGSD with the following parameters: minimum mapping quality (-minMapQ 30),
256 minimum base quality (-minQ 20), missing data (-minInd 95%), Global Depth (-setMaxDepth 600

257 * number of individuals), minimum genotype posterior probability (-postCutoff 0.95), single and
258 double-tons were accordingly removed based on minimum minor allele frequencies (-MinMaf),
259 anomalous reads (-remove_bads 1; SAM flag above 255), adjusted mapping quality for excessive
260 mismatches (-C 50), performed BAQ computation (-baq 1), minimum coverage for genotype
261 calling (-geno_minDepth 3), use of SAMtools genotype likelihood model (-GL 1), and estimated
262 posterior genotype probabilities assuming a uniform prior (-doPost 2). In addition, we used the
263 ANGSD SNP calling method (-SNP_pval 1e-6), where a Likelihood Ratio Test is used to compare
264 between the null (maf = 0) and alternative (estimated maf) hypotheses by using a X^2 distribution
265 with one degree of freedom.

266 2.4. Nuclear DNA phylogeny

267 Our first dataset (Dataset I) consisted of the full set of GBS sites (all sites recovered in our
268 library passing the filtering scheme - both constant and variable) from 48 *Kryptolebias* individuals
269 and *Nematolebias whitei* as an outgroup. This dataset consisted of 174,282 nuclear sites. We ran
270 the ModelFinder algorithm (Kalyaanamoorthy et al., 2017) implemented in IQ-Tree2 v. 2.1.0
271 (Minh et al., 2020) to infer the best optimal substitution model for the concatenated dataset. Then,
272 we ran IQ-Tree2 to infer the maximum likelihood (ML) tree for the concatenated alignment and
273 to assess the support of internal branches using the Shimodaira-Hasegawa-like procedure support
274 (SH-aLRT) (Guindon et al., 2010), the Bayesian-like transformation of SH-aLRT support (aBayes)
275 (Anisimova et al., 2011), and the ultrafast bootstrap support (UFBoot) (Hoang et al., 2018) with
276 1,000 replicates.

277 To visualize the most common phylogenetic signal between *Kryptolebias* species while
278 considering uncertainty that may derive from reticulation, we ran a NeighborNet analysis based
279 on uncorrected p-distances among individuals from Dataset II (115,397 GBS sites across 48

280 *Kryptolebias* samples with coverage between 4.77X and 444.95X (mean 153.48X) and missing
281 data per loci ranging from 0% to 1.83% (mean 0.25%); Supplementary Table S3) was conducted
282 in SplitsTree v. 4.18.2 (Huson and Bryant, 2006).

283 2.5. Phylogenetic networks and ancestral introgression analysis

284 The bifurcating nature of phylogenetic trees may not accurately describe the phylogenetic
285 history of a particular group, especially when introgression events are common (Olave and Meyer,
286 2020). Given the reduced representation nature of our GBS library and the high genetic divergence
287 between the freshwater (*K. brasiliensis* and *K. gracilis*) and the remaining *Kryptolebias* species,
288 we limited our introgression analysis to the species composing the ‘mangrove killifishes clade,’
289 namely *K. marmoratus*, *K. hermaphroditus* (Central and Southern clades), *Kryptolebias* sp. ‘ESP’
290 and *K. ocellatus*.

291 We used two approaches to assess reticulation and ancestral introgression events in
292 *Kryptolebias*. First, to evaluate the incidence of reticulation events across the *Kryptolebias*
293 phylogenetic tree, we used the *julia* package PhyloNetworks v. 0.14.2 (Solís-Lemus et al., 2017).
294 This package uses concordant factor tables to infer networks using pseudolikelihood under the
295 multispecies network coalescent model. SNP-based concordant factors were inferred using the
296 program SNPs2CFs v.1.4 (Olave and Meyer, 2020). SNPs2CFs requires phased and unlinked SNPs
297 data. We called SNPs for 33 individuals of the mangrove killifishes clade, following the
298 parameters described in the variant calling section. This call resulted in a dataset containing a total
299 of 9,532 SNPs (Dataset III). To phase the data, we limited our dataset to SNPs located only in the
300 24 chromosomes of the *K. hermaphroditus* reference genome, filtering out all SNPs located in
301 unplaced scaffolds. To minimize linkage amongst SNPs, we further filtered out our dataset to SNPs
302 separated by a minimum distance of five thousand base-pairs, resulting in a dataset containing

303 5,813 SNPs with an average distance of 110,809 base-pairs among SNPs (Dataset IV). We phased
304 this dataset using Beagle v. 5.2 (Browning et al., 2021) and generated concordance factors using
305 SNPs2CFs. The full number of quartets in our dataset is too large to be processed in
306 PhyloNetworks (Solís-Lemus et al., 2017). Therefore, we limited our sample to 1,000 alleles per
307 species quartet (n.quartets = 1,000 on SNPs2CFs), resulting in a total 5,000 quartets. We estimated
308 phylogenetic networks with a hmax (maximum number of hybridization events) value ranging
309 from zero to seven. Our starting network (hmax=0) was represented by a concatenated ML tree
310 ran on IQ-Tree2 using the full set of GBS loci (both constant and variable) for this dataset (Dataset
311 V – 1,631,872 nuclear sites with no missing data: Supplementary Figure S5). The resulting
312 network for each hmax value was used for every subsequent run. We plotted the log-
313 pseudolikelihood and selected the networks that resulted in substantial pseudolikelihood
314 improvements.

315 To further evaluate the evidence of ancestral introgression in *Kryptolebias*, we used the
316 software Dsuite v. 0.4 r28 (Malinsky et al., 2021) to calculate Patterson’s D statistics (ABBA-
317 BABA test) and f4-ratios (an estimate of admixture fraction). ABBA-BABA rely on comparisons
318 between bi-allelic SNPs for four taxa (e.g., T1, T2, T3, O) which are related to each other by a
319 rooted tree (e.g. (((T1, T2), T3), O)). ‘A’ and ‘B’ represents the ancestral and derived alleles,
320 respectively. Under a no gene flow scenario, the patterns of ABBA (sharing of alleles between T2
321 and T3) and BABA (sharing of alleles between T1 and T3) are expected to occur with equal
322 frequencies, while significant deviation from equal frequencies is consistent with introgression
323 between T3 and either T2 (ABBA) or T1 (BABA). We formally tested for three possible past
324 introgression events within the mangrove killifishes clades in *Kryptolebias* based on either
325 previous or current evidence: i) between *K. marmoratus* and *K. hermaphroditus* ‘Central clade’ as

326 suggested by Tatarenkov et al. (2018, 2021) with the following tree topology: (((Kher_South,
327 Kher_Central), Kmar), KspESP)); ii) between *K. hermaphroditus* ‘Southern clade’ and
328 *Kryptolebias* sp. ‘ESP’ (see results) with the following tree topology (((Kmar, Kher_South),
329 KspESP), Koce)); and between (iii) *K. hermaphroditus* ‘Southern clade’ and *K. ocellatus*, given
330 the ongoing hybridization found in Berbel-Filho et al. (2021) with the following tree topology: (((
331 Kher_South, KspESP), Koce), Kbra). ‘Kmar’, ‘Kher_Central’, ‘Kher_South’, ‘KspESP’, ‘Koce’,
332 and ‘Kbra’ refer to *K. marmoratus*, *K. hermaphroditus* ‘Central clade’, *K. hermaphroditus*
333 ‘Southern clade’, *Kryptolebias* sp. ‘ESP’, *K. ocellatus*, and *K. brasiliensis*, respectively. For the
334 first two introgression tests (i and ii), we used Dataset III while for test iii we called SNPs for a
335 dataset containing one representative per species (for maximize the number of sites given the
336 inclusion of *K. brasiliensis* as an outgroup) of the mangrove killifish clade and an individual of *K.*
337 *brasiliensis* as an outgroup (Dataset VI – 10,648 SNPs with no missing data).

338 2.6. Genetic structure of the mangrove killifishes clade

339 Our results indicated (see below) the existence of a previously unknown lineage of
340 *Kryptolebias* in a single coastal sampling site in of Espírito Santo State in Brazil (referred above
341 as *Kryptolebias* sp. ‘ESP’) (Supplementary Figure S4). We further explored the nuclear genomic
342 structure *Kryptolebias* sp. ‘ESP’ in comparison to the other lineages in the mangrove killifishes
343 clade (see Fig. 3) using Dataset III. To estimate individual ancestries, we used ngsAdmix v. 3.2
344 (Skotte et al., 2013) with K values ranging between 2–10 for 100 replicates using default
345 parameters, except for tolerance for convergence (-tol 1×10^{-6}), log likelihood difference in 50
346 iterations (-tolLike 50 1×10^{-3}), and a maximum number of EM iterations (-maxiter 10,000). We
347 used StructureSelector (Li and Liu, 2018) to estimate the most likely number of genetic clusters.
348 A pairwise genetic distance matrix between individual’s matrix was computed directly from the

349 genotype likelihoods using ngsDist v1.0.2 (Vieira et al., 2015) and was then used for
350 Multidimensional Scaling (MDS) using the R function *cmdscale*. To calculate heterozygosity, we
351 called the full set of GBS sites (both constant and variable) for a dataset containing all 33
352 individuals of the mangrove killifish clade (Dataset VII - 863,662 nuclear sites for 33 individuals
353 with 5% of missing data). We used ANGSD to compute the unfolded global estimate of the Site
354 Frequency Spectrum (SFS) using one individual of *K. brasiliensis* as the source of ancestral
355 sequence. Heterozygosity was calculated as the proportion of heterozygous sites by the total
356 number of sites per individual.

357 2.7. Introgression between *Kryptolebias* sp. ‘ESP’ and *K. hermaphroditus* ‘Southern clade’

358 To gain further insights into the structure of the hybrid zone between *Kryptolebias* sp.
359 ‘ESP’ lineage and *K. hermaphroditus* ‘Southern clade’ (as indicated in our results), we called SNPs
360 for a dataset containing only *Kryptolebias* sp. ‘ESP’ and *K. hermaphroditus* ‘Southern clade’
361 individuals (Dataset VIII – 5,688 SNPs for 18 individuals with no missing data). With this dataset,
362 we addressed the patterns of allele distribution (e.g., number of fixed and/or shared alleles)
363 between the two lineages.

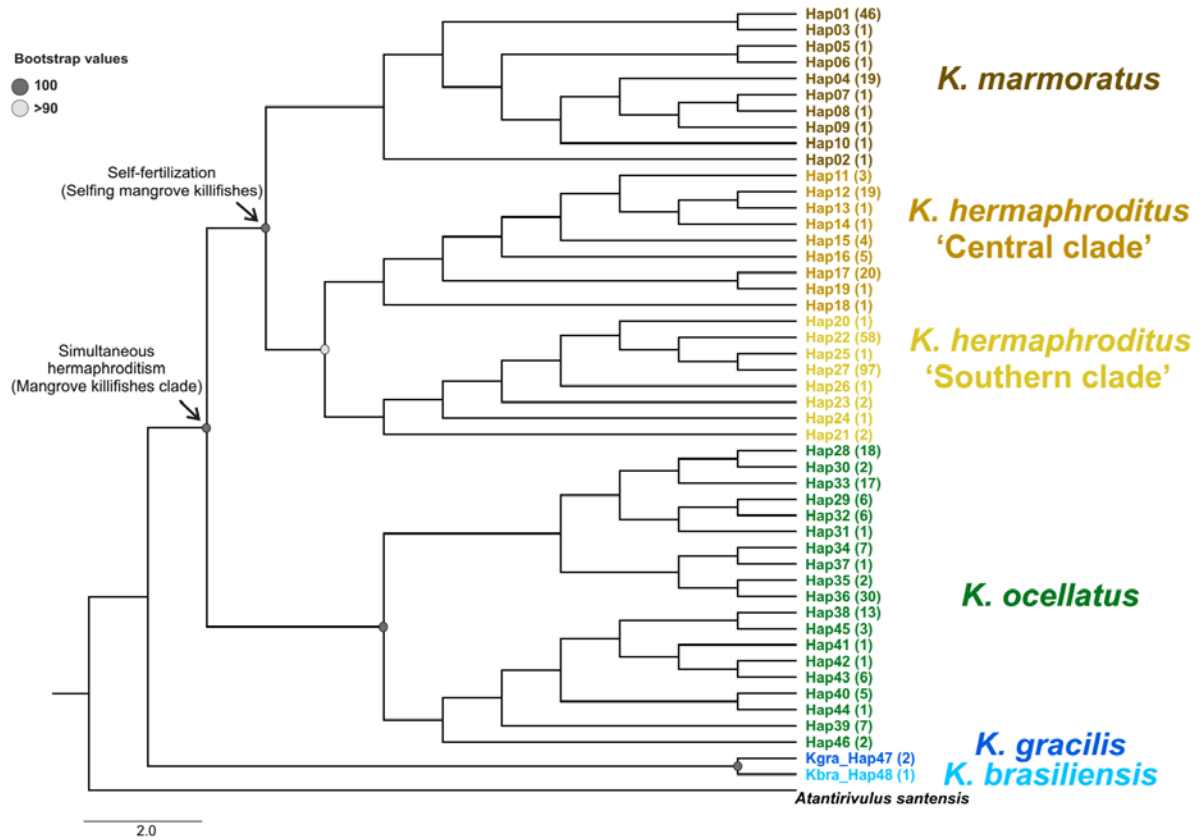
364 3. Results

365 3.1. Mitochondrial phylogeny

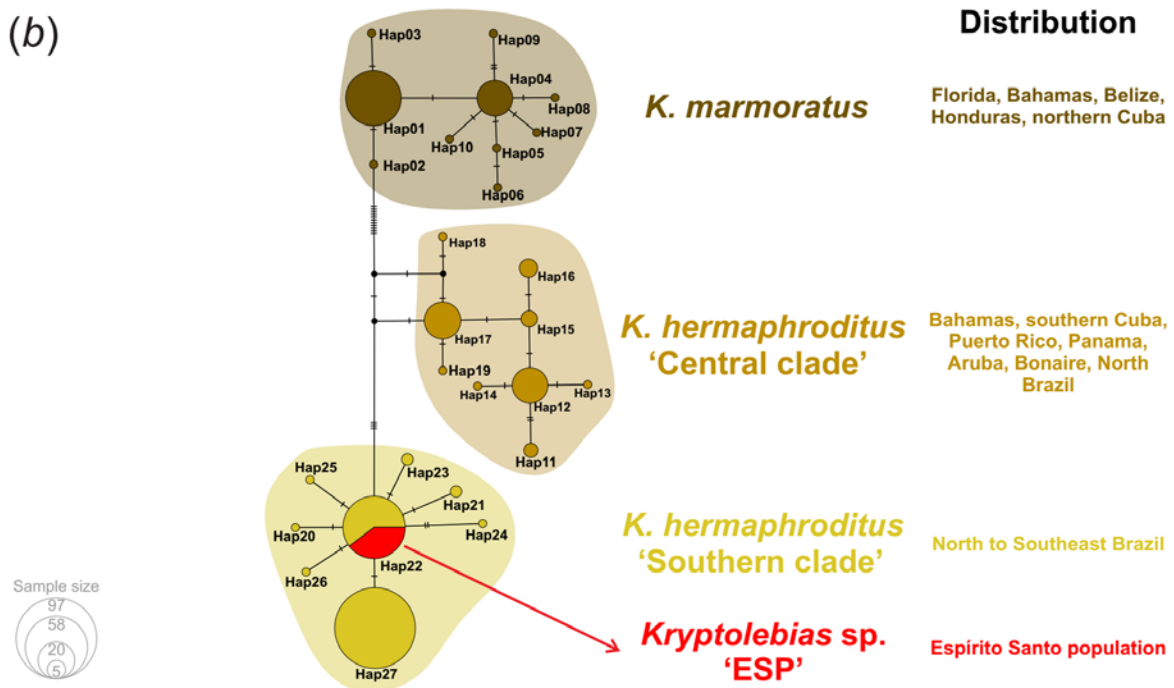
366 The phylogenetic reconstruction based on 49 unique *cox1* haplotypes extracted from 423
367 *Kryptolebias* individuals was largely consistent with previously suggested phylogenetic
368 relationships in the genus (Berbel-Filho et al., 2020; Costa, 2004; Costa, 2007; Costa et al., 2010;
369 Kanamori et al., 2016; Murphy et al., 1999; Tatarenkov et al., 2017; Tatarenkov et al., 2009;
370 Vermeulen and Hrbek, 2005) (Fig. 2a). The freshwater species *K. gracilis* and *K. brasiliensis*

371 formed a clade which is sister group of the mangrove killifishes clade, composed of *K. ocellatus*,
372 *K. hermaphroditus* and *K. marmoratus*. The latter two formed a well-supported clade within the
373 mangrove killifishes clade (the selfing mangrove killifishes). As previously indicated, there were
374 two *K. hermaphroditus* mtDNA clades, one comprising samples from San Salvador Island, the
375 Caribbean and northern portions of South America (the ‘Central clade’ in Tatarenkov et al. 2017
376 and Lira et al. 2021), and another composed of samples from Northeast and Southeast Brazil (the
377 ‘Southern clade’ in Tatarenkov et al. 2017 and Lira et al. 2021). All the 23 individuals from the
378 Espírito Santo locality exhibited a single *cox1* haplotype (Hap22, Fig 2), which is widespread in
379 many *K. hermaphroditus* populations along approximately 2,600km of the Northeast and
380 Southeast regions of the Brazilian coast (Lira et al., 2021) (Fig. 2b).

(a)



(b)

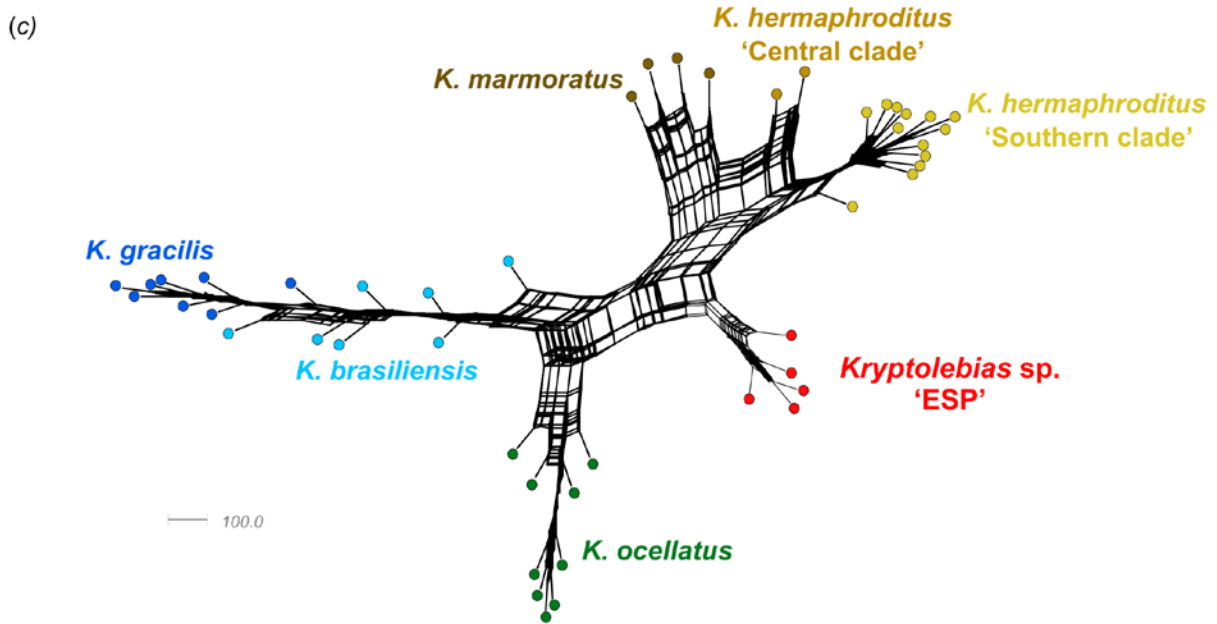
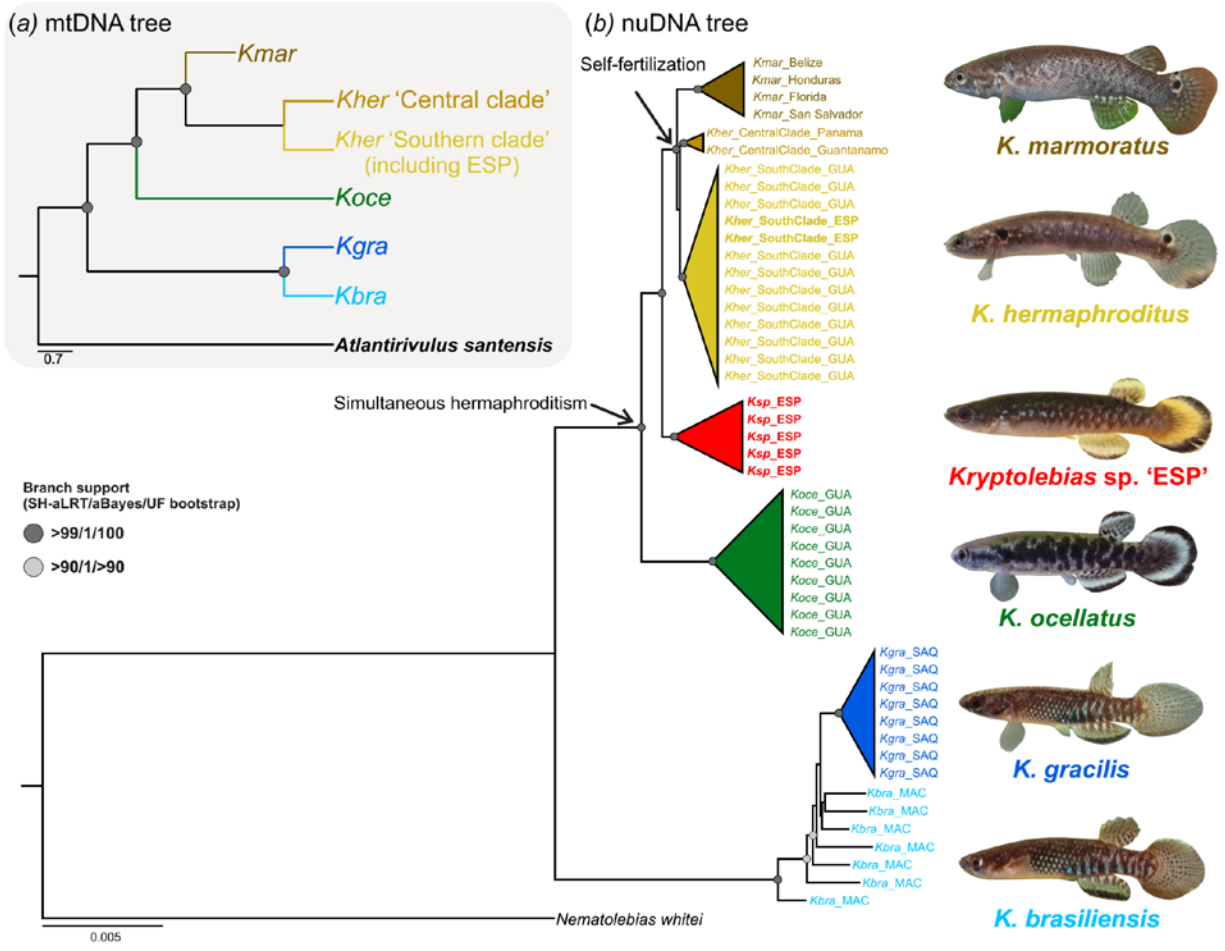


382 **Figure 2.** Maximum-likelihood reconstruction for 49 unique *cox1* haplotypes extracted from 423
383 *Kryptolebias* individuals. (a) Full tree containing the relationships among the 49 haplotypes with
384 tip labels colored by species/lineages names. Tip labels show haplotypes and number of
385 individuals sequenced (in parenthesis). (b) Haplotype network for the 27 *cox1* haplotypes for
386 individuals belonging to the selfing mangrove killifishes clade with their respective distribution.
387 Details for all samples used for these analyses are provided in Table S1.

388 3.2. Nuclear Phylogeny

389 Our ML phylogenetic reconstruction based on 174,282 nuclear DNA sites (Dataset I) from 48
390 *Kryptolebias* individuals was generally concordant with the phylogenetic relationships proposed
391 in the mtDNA tree, with two main exceptions (Fig. 3b). Although the freshwater species *K. gracilis*
392 and *K. brasiliensis* grouped together, samples from the former formed a monophyletic group
393 within a non-monophyletic composed of *K. brasiliensis* samples. The other exception consisted of
394 a previously unknown and well-supported clade containing five individuals from the Espírito
395 Santo locality. This clade (hereafter named as *Kryptolebias* sp. ‘ESP’) formed a sister clade to the
396 selfing mangrove killifishes, consisting of *K. marmoratus* and *K. hermaphroditus* (both Central
397 and Southern clades). Two additional individuals from the Espírito Santo locality clearly belonged
398 to *K. hermaphroditus* ‘Southern clade’, suggesting this population consisted of two sympatric
399 species. All 23 individuals sequenced for mtDNA from Espírito Santo locality (including the five
400 *Kryptolebias* sp. ‘ESP’ individuals) had the same mtDNA haplotype typically observed in *K.*
401 *hermaphroditus* populations in Northeast and Southeast Brazil (Hap22, Fig. 2), representing a clear
402 case of mito-nuclear discordance in *Kryptolebias*. Our phylogenetic network reconstruction using
403 SplitsTree largely agreed with the lineages found in our mtDNA and ML phylogenetic
404 reconstruction (Figs 2a and 3b). However, it also indicated the highest levels of site tree

405 discordance in *Kryptolebias* are within the mangrove killifish clade (Fig. 3c). This finding suggests
406 events of introgression may have been common during the evolutionary history of this clade.



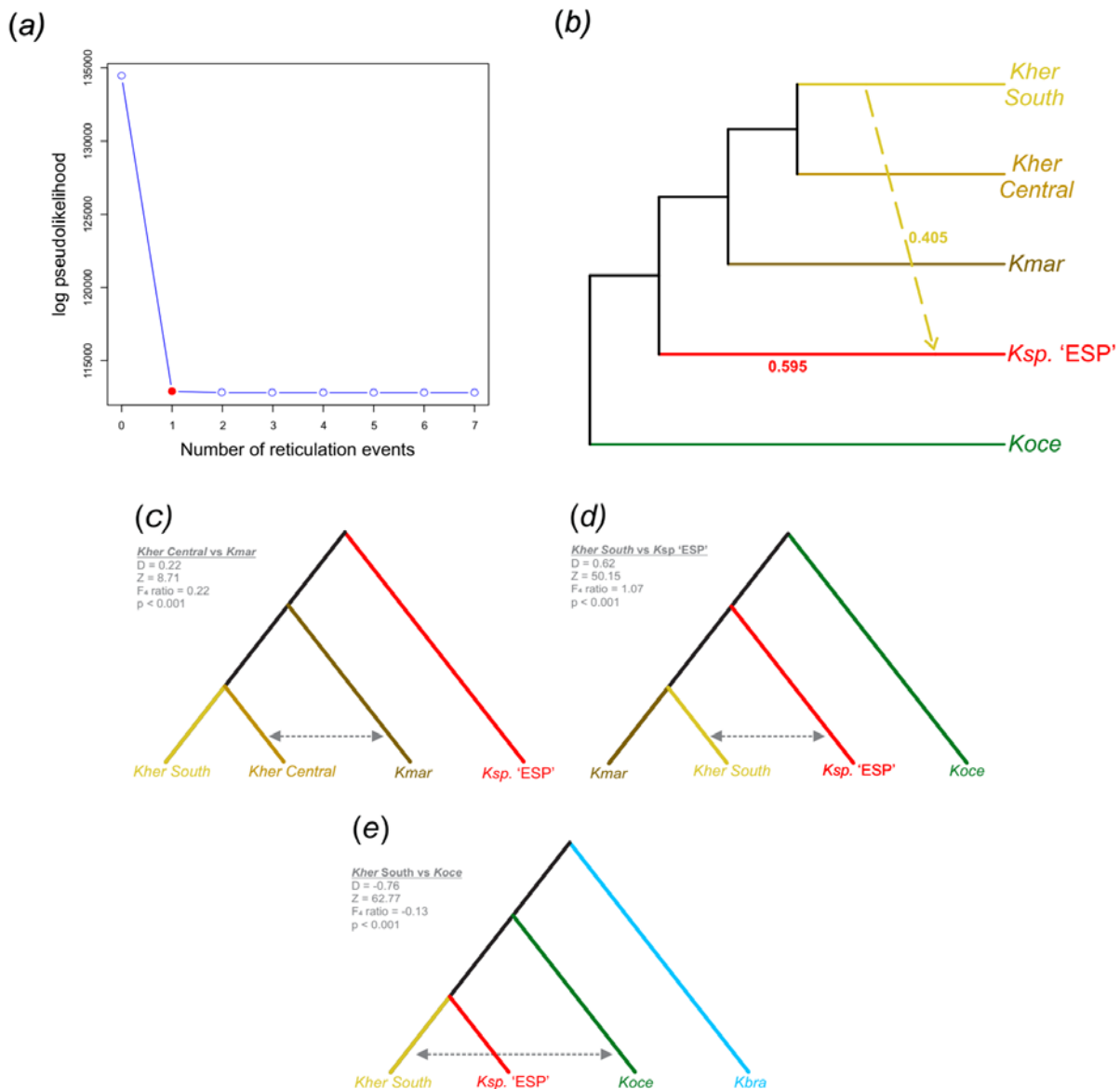
408 **Figure 3.** Phylogenetic reconstructions of the genus *Kryptolebias* using IQ-Tree 2 v. 2.0.1. (a)
409 Schematic representation of the maximum-likelihood phylogenetic tree based on 49 unique
410 mtDNA *cox1* haplotypes extracted from 423 *Kryptolebias* individuals. Node circles represent
411 nonparametric bootstrap values = 100. The full mtDNA phylogenetic reconstruction is provided
412 on Figure 2. (b) Maximum-likelihood phylogenetic tree based on 174,842 GBS nuclear sites
413 (Dataset I). Node circles represent SH-aLRT (%), aBayes, and ultrafast bootstrap (%) support
414 values, respectively. Only nodes with high support (SH-aLRT ≥ 90 , aBayes = 1, and ultrafast
415 bootstrap > 90) are shown. Branch lengths are shown in substitutions per site. Intraspecific clades
416 were collapsed to facilitate visualization. The full nuclear phylogenetic reconstruction is provided
417 on Supplementary Fig. S4. (c) 95% confidence phylogenetic network (Neighbor-Net) constructed
418 using SplitsTree based on all sites from Dataset II. All species, with exception of *K. marmoratus*
419 and *K. hermaphroditus* (represented by hermaphrodites), are represented in the figure by male
420 individuals.

421 3.3. Phylogenetic networks and ancestral introgression

422 Our PhyloNetworks analysis indicated that the largest improvement in pseudolikelihood
423 scores across the number of reticulation events evaluated (ranging from 1 to 7) occurred between
424 zero (the original tree) and one reticulation event (Fig. 4a). The network generated with one
425 reticulation indicated ancestral introgression from *K. hermaphroditus* ‘Southern clade’ and
426 *Kryptolebias* sp. ‘ESP’, with the latter as hybrid lineage inheriting 40% of its genomic content
427 from the former, despite the fact these two lineages are relatively far from each other in the
428 phylogenetic tree (Fig. 4b).

429 Introgression events between *K. hermaphroditus* ‘Central clade’ and *K. marmoratus* ($D =$
430 0.22 ; Z -score = 8.71; F_4 ratio = 0.22; $p < 0.001$) (Fig. 4c), between *K. hermaphroditus* ‘Southern

431 clade' and *Kryptolebias sp.* 'ESP' ($D = 0.62$; Z -score = 50.15; F_4 ratio = 1.07; $p < 0.001$) (Fig. 4d)
 432 and between *K. hermaphroditus* 'Southern clade' and *K. ocellatus* ($D = -0.76$; Z -score = 62.77; F_4
 433 ratio = -0.13; $p < 0.001$) (Fig. 4e) were all confirmed by our ABBA-BABA test, revealing
 434 extensive introgression events in several *Kryptolebias* lineages.



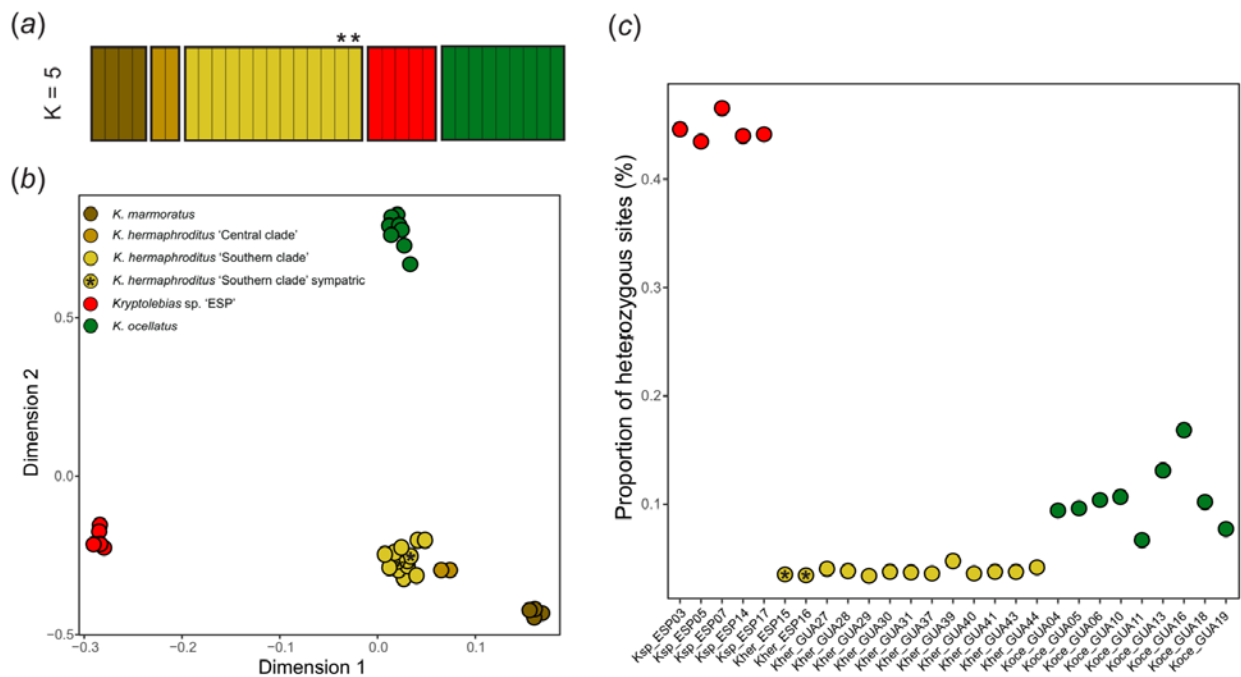
435
 436 **Figure 4.** Phylogenetic networks and introgression analysis in the mangrove killifishes clade.
 437 Genetic structure analysis for mangrove killifish species based on 9,532 SNPs (Dataset III). (a)

438 Log-pseudolikelihood scores per number of reticulation events tested using PhyloNetworks v.
439 0.14.2 (Solís-Lemus et al., 2017). The red dot indicates the network chosen based on a large
440 improvement of the pseudolikelihood score. (b) Phylogenetic network with one reticulation event.
441 Numbers indicate inheritance proportions in the hybrid lineage. (c-e) ABBA-BABA results for
442 introgression tests between: (c) *K. hermaphroditus* ‘Central clade’ (*Kher Central*) and *K.*
443 *marmoratus* (*Kmar*); (d) *K. hermaphroditus* ‘Southern clade’ (*Kher South*) and *Kryptolebias*
444 sp. ‘ESP’ (*Ksp. ESP*); (e) *K. hermaphroditus* ‘Southern clade’ (*Kher South*) and *K. ocellatus*
445 (*Koce*).

446 3.4. Genetic structure of the mangrove killifishes clade

447 Admixture analysis indicated the presence of five genetic clusters (Fig 4a), each representing
448 the mangrove killifish clade lineages recovered by the phylogenetic reconstruction based on
449 nuclear sites (Fig. 2b). All four metrics generated by StructureSelector further suggested five as
450 the most likely number of genetic clusters (Supplementary Fig. S7; all clusters shown in
451 Supplementary Fig. S8). As also indicated by our phylogenetic reconstruction, the Espírito Santo
452 population is composed of two highly different lineages at the nuclear genome, with two of the
453 individuals sequenced belonging to *K. hermaphroditus* ‘Southern clade’, and the remaining five
454 belonging to the previously unknown lineage *Kryptolebias* sp. ‘ESP’, despite the fact that all those
455 individuals (and other 18 individuals sequenced from the same population) have the same mtDNA
456 haplotype (Hap22 in Fig. 2) commonly found in individuals from the *K. hermaphroditus* ‘Southern
457 clade’ in Northeast and Southeast Brazil. Our admixture analysis further indicated that these two
458 lineages are quite differentiated from each other, with no evidence of current admixture (or early
459 hybrid generation individuals) between them (Fig. 5a). This result can also be observed in our
460 MDS analysis (Fig. 5b), in which the clusters representing the species (with exception of *K.*

461 *hermaphroditus* Central and Southern clades – highlighting the proximity between these two
 462 lineages) occupied different portions of the eigenspace, with *Kryptolebias* sp. ‘ESP’ and *K.*
 463 *hermaphroditus* occupying opposite sides of the first dimension of genetic distance variation . In
 464 terms of genetic diversity, *Kryptolebias* sp. ‘ESP’ individuals had in average 4.25x higher
 465 proportion of heterozygous sites (average: 0.45) than the outcrossing species *K. ocellatus* (average:
 466 0.10), and 11.7x higher than the selfing (and sympatric) *K. hermaphroditus* ‘Southern clade’
 467 (average: 0.04) (Fig. 5c). Possibly due to long-term generation of selfing and/or low-coverage
 468 nature of sequencing, *K. marmoratus* and *K. hermaphroditus* ‘Central clade’ individuals had an
 469 extremely low proportion of heterozygous sites (< 0.001) across the GBS sites sampled in Dataset
 470 VII.



471
 472 **Figure 5.** Genetic structure plots for the lineages in the mangrove killifish clade. (a) Admixture
 473 plot for K=5, indicated by StructureSelector (Li and Liu, 2018) as the most likely number of
 474 genetic clusters based on Dataset III (9,532 SNPs). (b) Multidimensional scaling plot based on the

475 pairwise genetic distances between individuals extracted from Dataset III. (c) Proportion of
476 heterozygous sites per individual based on the site frequency spectrum for Dataset VII (863,662
477 nuclear sites). For ease of visualization, species based on data extracted from whole-genome
478 sequences (*K. marmoratus* and *K. hermaphroditus* ‘Central clade’) were omitted from the plot
479 given a very low number of heterozygous sites (see Results). All plots follow the color scheme
480 described in (b). Across all plots, individuals marked with asterisks represent *K. hermaphroditus*
481 ‘Southern clade’ sympatric to *Kryptolebias* sp. ‘ESP’.

482 3.5. Introgression between *Kryptolebias* sp. ‘ESP’ and *K. hermaphroditus* ‘South clade’

483 Out of 5,688 SNPs in Dataset VIII, 4,976 (87.48%) are fixed and homozygous across all 13 *K.*
484 *hermaphroditus* ‘Southern clade’ individuals, reflecting the highly selfing nature of the species.
485 Out of those, 4,186 (84.12%) SNPs are present in a heterozygous state in *Kryptolebias* sp. ‘ESP’,
486 another strong indication that the genome of *K. hermaphroditus* ‘Southern clade’ introgressed into
487 the genome of a previously unknown *Kryptolebias* lineage, resulting in *Kryptolebias* sp. ‘ESP’.
488 This latter lineage is highly heterozygous (4,714 out of 5,688 (82.87%) SNPs are heterozygote).
489 Further indication that an unknown and highly differentiated species was originally involved in
490 the introgression with individuals of the *K. hermaphroditus* ‘Southern clade’ is the fact that
491 74.68% (4,248 out of 5,688) of the SNPs contained alleles exclusive to individuals of *Kryptolebias*
492 sp. ‘ESP’.

493 4. Discussion

494 Our study provided the first phylogenomic-based hypothesis for the phylogenetic relationships
495 within killifish genus *Kryptolebias*, involving five out of the seven currently valid species. Our
496 results (based on both mtDNA and nuclear markers) largely agreed with previously proposed
497 phylogenetic relationships within the genus, comprising two major monophyletic groups: one

498 grouping the freshwater fishes (*K. brasiliensis* and *K. gracilis*), while the other grouping the
499 ‘mangrove killifish clade’, comprising *K. ocellatus*, *K. hermaphroditus* (Central and Southern
500 clades) and *K. marmoratus* (Berbel-Filho et al., 2020; Costa et al., 2010; Murphy et al., 1999;
501 Tatarenkov et al., 2017; Tatarenkov et al., 2009; Vermeulen and Hrbek, 2005). In addition, our
502 results revealed an extensive history of introgression in *Kryptolebias*. Our findings revealed yet a
503 highly differentiated (and previously unknown) lineage with elevated levels of heterozygosity and
504 a history of admixture with the predominantly-selfing and sympatric *K. hermaphroditus*.

505 4.1. *Kryptolebias* phylogenetic relationships and introgression

506 Previous attempts to reconstruct the phylogenetic relationships within *Kryptolebias* were
507 based either exclusively on mtDNA (Vermeulen and Hrbek, 2005), and/or were exclusively
508 focused on the ‘mangrove killifish clade’ (Berbel-Filho et al., 2020; Kanamori et al., 2016; Murphy
509 et al., 1999; Tatarenkov et al., 2017; Tatarenkov et al., 2009; Weibel et al., 1999). Our phylogenetic
510 reconstruction not only expanded the number of genomic loci used, but also widened the
511 taxonomic sampling of *Kryptolebias*, particularly by including the freshwater species: *K. gracilis*
512 and *K. brasiliensis*; representatives of recently uncovered lineages (*K. hermaphroditus* Central and
513 Southern clades); and a lineage revealed by the present study (*Kryptolebias* sp. ‘ESP’). Overall,
514 our phylogenetic reconstruction generally agrees with the topologies previously proposed by
515 Vermeulen and Hrbek (2005) based on mtDNA loci, where two monophyletic *Kryptolebias* clades
516 were represented by species living in freshwater streams or brackish environments close to
517 mangrove forests (the freshwater clade and mangrove killifishes clade, respectively). Although we
518 have not sampled the Amazonian freshwater species *K. sepia* and *K. campelloi*, those species are
519 thought to be closely related to *K. brasiliensis* (Costa, 1990; Vermeulen and Hrbek, 2005), which
520 in our phylogeny grouped together with *K. gracilis* in the ‘freshwater clade’. It is important to

521 highlight that our *K. brasiliensis* samples have not formed a monophyletic clade within the
522 freshwater clade of our nuclear phylogeny, with *K. gracilis* being nested within *K. brasiliensis*
523 (Fig. 3b) Those two species are morphologically very similar, with *K. brasiliensis* being distributed
524 in broader area along lowland streams and creeks in the state of Rio de Janeiro (Costa 2007). Our
525 study thus calls for further research on the taxonomic status of *K. brasiliensis* and *K. gracilis*, with
526 the possibility of the former representing a species complex.

527 Our nuclear phylogeny revealed some differences from previous reconstructions within the
528 mangrove killifishes clade. So far, all studies that tried to reconstruct the phylogenetic relationships
529 within this clade, regardless of whether it was based on mtDNA (Berbel-Filho et al., 2020; Murphy
530 et al., 1999; Tatarenkov et al., 2017; Tatarenkov et al., 2009; Vermeulen and Hrbek, 2005; Weibel
531 et al., 1999) or nuclear markers (Kanamori et al., 2016), have supported the obligated outcrossing
532 species *K. ocellatus* (Berbel-Filho et al., 2020) as the sister-species of the clade containing the
533 selfing species (*K. marmoratus* and *K. hermaphroditus*). Our phylogenetic reconstruction revealed
534 a clear case of mito-nuclear discordance (see discussion below) including a previously unknown
535 lineage more closely related to the selfing mangrove killifishes than to *K. ocellatus*. This change
536 in topology may have implications for understanding the evolution of mating systems within the
537 genus. As all the other known *Kryptolebias* species are dioecious and inhabit freshwater habitats,
538 the classical view based on the phylogenetic mapping of reproductive traits in *Kryptolebias*
539 suggested that synchronous hermaphroditism has emerged in the common ancestor of all
540 mangrove killifish species (*K. ocellatus*, *K. hermaphroditus* and *K. marmoratus*), with the self-
541 fertilization evolving later in the common ancestor of the sister-species *K. hermaphroditus* and *K.*
542 *marmoratus* (Awise and Tatarenkov, 2015; Costa et al., 2010). However, the phylogenetic
543 positioning of *Kryptolebias* sp. 'ESP' as the sister-group of the selfing species raises the discussion

544 of whether self-fertilization may have evolved earlier in the genus. Notwithstanding, it is important
545 to note that self-fertilization tends to reduce heterozygosity levels in half every generation (Avisé,
546 2008). The fact that the individuals from *Kryptolebias* sp. ‘ESP’ examined here had over 11x
547 higher level of heterozygosity when compared to *K. hermaphroditus*, together with the evidence
548 of ancestral introgression from *K. hermaphroditus* ‘Southern clade’ into *Kryptolebias* sp. ‘ESP’,
549 suggests that *Kryptolebias* sp. ‘ESP’ may not undergo self-fertilization. All non-male individuals
550 captured in the sampling locality of *Kryptolebias* sp. ‘ESP’ (and previously by Costa 2016) had a
551 typical external appearance of hermaphrodites of the selfing mangrove killifishes, suggesting this
552 may be another androdioecious, but not self-fertilizing, species in the genus, similarly to *K.*
553 *ocellatus* (Berbel-Filho et al., 2020). Nonetheless, our limited sample size makes imperative the
554 need for further life-history and behavioural evaluation of the mating system of *Kryptolebias* sp.
555 ‘ESP’ individuals. Until then, the possibility that self-fertilization may have evolved earlier (in the
556 common ancestor between *Kryptolebias* sp. ‘ESP’, *K. hermaphroditus*, and *K. marmoratus*) in
557 *Kryptolebias* must be considered.

558 Another major goal of our study was to evaluate the possibility that reticulate evolution
559 may have played a role in the diversification of the genus *Kryptolebias*. Our phylogenetic networks
560 analyses showed complex history of reticulate evolution in the mangrove killifish clade (Fig. 3c),
561 and revealed an ancient introgression event from *K. hermaphroditus* ‘Southern clade’ into
562 *Kryptolebias* sp. ‘ESP’. This reticulation event may explain the fact that all individuals of
563 *Kryptolebias* sp. ‘ESP’ had high heterozygosity levels and the same mtDNA haplotype commonly
564 found in *K. hermaphroditus* ‘Southern clade’ in Northeast Brazil. Contrary to the prediction that
565 highly-selfing taxa (such as *K. hermaphroditus*) provide a low opportunity for hybridization and
566 introgression (Pickup et al., 2019), this ancestral reticulation event suggests that hermaphrodites

567 of the *K. hermaphroditus* lineage played the maternal role in introgression events with a previously
568 unknown lineage, now evident in the genome of *Kryptolebias* sp. ‘ESP’. Tatarenkov et al. (2021)
569 found bi-directional hybridization between two highly selfing strains of *K. marmoratus* and *K.*
570 *hermaphroditus* ‘Central clade’, while Berbel-Filho et al. (2021) also found a single backcross
571 between an F1 individual and *K. hermaphroditus* ‘Southern clade’ in Southeast Brazil. Taken
572 together, these results suggest that although rare, opportunities to outcross and hybridize with the
573 selfing *Kryptolebias* may occasionally occur. Backcrossing between F1 individuals and males of
574 the *Kryptolebias* sp. ‘ESP’ lineage may have then further contributed to the movement of genomic
575 DNA from *K. hermaphroditus* ‘Southern clade’ into *Kryptolebias* sp. ESP. The fact that we only
576 found individuals with *K. hermaphroditus* ‘Southern clade’ mtDNA hints at the possibility of local
577 extinction of individuals with the mtDNA of *Kryptolebias* sp. ‘ESP’, however we acknowledge
578 that testing of this hypothesis requires further sampling in the area. The question of whether ‘pure’
579 *Kryptolebias* sp. ‘ESP’ individuals still exist or evidence for this (possibly extinct) lineage can
580 only be found in extant admixed populations with *K. hermaphroditus* is open to investigation. Thus
581 far, the closest sampling site around the Espírito Santo locality (only 5 km apart from Coqueiral
582 Beach, where *Kryptolebias* sp. ‘ESP’ was found) had mtDNA haplotypes and hermaphrodite
583 appearance commonly found in *K. hermaphroditus* (Lira et al., 2021).

584 The single reticulation event found in our phylogenetic networks analysis seems to
585 contradict the finding of multiple introgression events using site patterns counts (ABBA-BABA
586 tests) found between *Kryptolebias* lineages of the mangrove killifishes clade. However, these two
587 types of introgression tests tend to recover introgression events at different time scales. ABBA-
588 BABA test assumes that multiple substitutions at a particular site are rare or do not occur, as many
589 substitutions at individual sites could affect the patterns of site discordance. This assumption tends

590 to not hold true for deeply diverged taxa (Hibbins and Hahn, 2022). Therefore, ABBA-BABA tests
591 are usually more suitable for testing more recent introgression events. Phylogenetic networks, on
592 the other hand, use discordance between gene trees and/or concordant factors, being thus less
593 impacted by the multiple substitutions at individual sites, making them more suitable for
594 estimating ancestral introgression events (Hibbins and Hahn, 2022). While we only found evidence
595 for one reticulation event from *K. hermaphroditus* ‘Southern clade’ into *Kryptolebias* sp. ‘ESP.’
596 in our phylogenetic network using PhyloNetworks, our phylogenetic network visualization using
597 SplitsTree revealed many tree discordances in the mangrove killifish clade, which is indicative of
598 potential introgression. Our genome-wide ABBA-BABA tests further confirmed that indication,
599 with evidence of introgression in the hybrid zones recently described between *K. marmoratus* and
600 *K. hermaphroditus* ‘Central clade’ (Tatarenkov et al., 2021), between *K. hermaphroditus*
601 ‘Southern clade’ and *K. ocellatus* (Berbel-Filho et al. 2021), and finally a significant signal of
602 introgression in the hybridization found here between *K. hermaphroditus* ‘Southern clade’ and
603 *Kryptolebias* sp. ‘ESP’. In addition to the assumption of low substitutions per site, it is also
604 important to acknowledge here another caveat of ABBA-BABA tests, which is the assumption of
605 no ancestral population structure in the ancestor between P1, P2 and P3 (Hibbins and Hahn, 2022).
606 If present, ancestral population structure can result to similar deviations of site patterns counts as
607 the ones caused by real introgression events (Eriksson and Manica, 2012). Despite those
608 limitations, overall, our findings suggest that introgressive events in *Kryptolebias* are common,
609 both at ancestral and/or recent time scales. Considering the possibility that both lineages of *K.*
610 *hermaphroditus* (Central and Southern clades) may belong to the same species (Lira et al., 2021)),
611 our results indicate that *K. hermaphroditus* has been involved in at least three different
612 introgression events with other *Kryptolebias* species across its range. Although ABBA-BABA

613 tests cannot evaluate the direction of introgression, these findings challenge the idea that highly-
614 selfing taxa provide low opportunities for hybridization and introgression in the long-term (Berbel-
615 Filho et al., 2021; Pickup et al., 2019).

616 4.2. The mysterious *Kryptolebias* sp. ‘ESP’ lineage

617 Given the unusually high frequency of males and their unique external coloration, we
618 sampled in the same locality (Coqueiral Beach, in Aracruz, Espírito Santo (Supplementary Figure
619 S1)) described in Costa (2016) to grasp further insights on the taxonomic status of this population.
620 In total, we sampled 46 *Kryptolebias* individuals from this sampling locality, three of them could
621 be identified based on external coloration as *K. hermaphroditus* males according to Costa (2016).
622 All other non-male individuals captured in this sampling locality had the typical external
623 appearance of hermaphrodites of *K. hermaphroditus*, as also reported by Costa (2016). However,
624 our results revealed that in this locality two clearly differentiated *Kryptolebias* lineages/species
625 coexist. The fact that the *Kryptolebias* sp. ‘ESP’ lineage was only found in a case of mito-nuclear
626 discordance with *K. hermaphroditus*, calls for attention to the possibility of a cryptic species of
627 *Kryptolebias* in the region. In fact, Sarmiento-Soares et al. (2014) found two *Kryptolebias*
628 populations in other coastal streams in the state of Espírito Santo. Those individuals were initially
629 identified as *K. ocellatus*. Later, Costa (2016) collected individuals from Coqueiral beach (the
630 same locality sampled here) and identified them as *K. hermaphroditus*. Our analyses did not find
631 any evidence that individuals from Coqueiral Beach are *K. ocellatus*, however they add another
632 syntopic *Kryptolebias* lineage currently coexisting with *K. hermaphroditus* in Coqueiral Beach.
633 In addition, Costa (2016) used the male coloration found on males from this locality (together with
634 another locality in Rio de Janeiro state) to generally describe the coloration of *K. hermaphroditus*
635 males. While his description of male coloration is detailed and accurate, there are clear differences

636 in coloration between the *K. hermaphroditus* males found by Berbel-Filho et al. (2016), other
637 males sampled in different localities within the species range (Amorim et al. (2022);
638 Supplementary Figure S1) and the ones described in Costa (2016). Although we do not have
639 nuclear data for male individuals from this population, the evidence presented here for
640 *Kryptolebias* sp. ‘ESP’ prompts for further taxonomical evaluation on the identity of males from
641 this population, especially whether the males described in Costa (2016) represented males of
642 *Kryptolebias* sp. ‘ESP’ or *K. hermaphroditus* (or both).

643 Another striking feature of the hybrid zone between *Kryptolebias* sp. ‘ESP’ and *K.*
644 *hermaphroditus* in Coqueiral Beach is the evidence that despite the two species have exchanged
645 DNA in the past and are currently syntopic, there is no apparent evidence of current gene flow
646 between them (e.g., no F1s or early hybrid generations). Although we acknowledge our small
647 sampling size for this population, this scenario may suggest a strong mechanism of pre and/or
648 postzygotic reproductive isolation between the two sympatric lineages. Alternatively, we cannot
649 fully rule out the possibility that the two individuals of *K. hermaphroditus* in Coqueiral beach
650 found here represent a recent case of secondary contact, given the high heterozygosity found in
651 *Kryptolebias* sp. ‘ESP’ together with the evidence from recent phylogeographic studies indicating
652 that *K. hermaphroditus* has been dispersing southwards along the mangrove forests in the Brazilian
653 coast recently (Berbel-Filho et al., 2020; Lira et al., 2021; Tatarenkov et al., 2011; Tatarenkov et
654 al., 2017). Overall, the evolutionary history of *Kryptolebias* sp. ‘ESP’, its potential distribution, as
655 well its historical and current relationship with *K. hermaphroditus* is now open for investigation,
656 with putative scenarios such as hybrid speciation involving *K. hermaphroditus* and a previously
657 unknown (and possibly extinct) lineage, ancestral introgression involving a yet unknown lineage,

658 as fruitful lines of research to understand the origins of the mysterious *Kryptolebias* sp. ‘ESP’
659 lineage.

660 **5. Conclusion**

661 Introgression is the most common cause of mito-nuclear phylogenetic incongruences
662 among taxa (Toews and Brelsford, 2012). Our phylogenetic reconstruction using mtDNA and
663 genome-wide nuclear sites for the genus *Kryptolebias* generally agreed with previous
664 reconstructions but yielded different topologies for the same set of species. Such discordance
665 seems to have been caused by past introgression events in the genus. More importantly, our nuclear
666 reconstruction recovered a cryptic *Kryptolebias* lineage hidden behind the case of mito-nuclear
667 discordance. The striking example of mito-nuclear discordance found here (with an unknown
668 lineage having the same mtDNA haplotype of the introgressing lineage) highlights the need of
669 using multiple genomic regions (particularly with different genomic, levels of recombination and
670 inheritance properties) when reconstructing phylogenetic histories and making taxonomic
671 inferences in clades where introgression is relatively common, such as *Kryptolebias*.

672 **CRedit authorship contribution statement**

673 **Waldir M. Berbel-Filho:** Conceptualization, Methodology, Software, Formal Analysis,
674 Investigation, Resources, Data Curation Writing – original draft, Writing – review & editing,
675 Funding acquisition, Visualization. **George Pacheco:** Methodology, Software, Formal Analysis.
676 Writing – review & editing. **Andrey Tatarenkov:** Resources, Writing – review & editing. **Mateus**
677 **G. Lira:** Resources, Writing – review & editing. **Carlos Garcia de Leaniz:** Resources, Funding
678 acquisition, Supervision, Writing – review & editing. **Carlos M. Rodríguez-López:**
679 Methodology, Software Writing – review & editing. **Sergio M. Q. Lima:** Resources, Funding

680 acquisition, Supervision, Writing – review & editing. **Sofia Consuegra**: Resources, Funding
681 acquisition, Supervision, Writing – review & editing, Project Administration.

682 **Declaration of competing interests**

683 The authors declare no conflict of interest.

684 **Acknowledgements**

685 We are grateful to Dr. Helder Espírito-Santo for help during fieldwork. We thank Dr. Andrew
686 Thompson for discussions on the phylogenetic reconstruction. We are also grateful to Frans
687 Vermeulen for providing great pictures of live *K. marmoratus* individuals.

688 **Funding**

689 This work was supported by National Geographic/Waite program [W461-16], The Fisheries
690 Society of the British Isles (FSBI) through the small research grant program, and the Conselho
691 Nacional de Desenvolvimento Científico e Tecnológico (CNPq) [233161/2014-7]. C.M.R.L. was
692 partially supported by AFRI competitive grants [grant no. 2019-67013-29168/project accession
693 no. 1018617; grant no. 2021-67019-34606/project accession no. 1025891] and USDA National
694 Institute of Food and Agriculture, United States Department of Agriculture, Hatch Program project
695 no. KY011050/Accession No. 1020852. S. M. Q. L. receive CNPq Research Productivity Grants
696 (313644/2018-7).

697 **Data accessibility**

698 The 21 additional *coxI* sequences generated for this study are available at GenBank (access
699 numbers: OM962875-OM962895). Merged FastaQ files generated for this study can be found at
700 accessed at NCBI (accession PRJNA815481). FastaQ files for the samples of *K. hermaphroditus*
701 and *K. ocellatus* generated in Berbel-Filho et al. (2021) and used here can be accessed at NCBI

702 (accession PRJNA563625). All scripts used in the project are available at:
703 <https://github.com/waldirmbf/KryptolebiasGenomics>.

704 **Supplementary data**

705 **Table S1.** Sampling size, localities, and respective geographical coordinates for the 423
706 individuals included in the mtDNA phylogenetic reconstruction. ‘Reference’ refers to the study
707 where *cox1* sequences were extracted from. mtDNA haplotype refers to the haplotype numbers in
708 Figure 2 found for each sampling locality.

709 **Table S2.** Sampling locations and sizes for samples included in analysis. ‘ES’ and ‘RJ’ denote the
710 Brazilian states of Espírito Santo and Rio de Janeiro, respectively. ‘Reference’ refers to the source
711 of samples for the genomic analysis. Geographical coordinates for the additional whole-genome
712 samples included in the analysis were not provided in the original references. When present, names
713 in parenthesis refer to samples belonging to the same sampling locations as the mtDNA samples
714 described in Table S1. Asterisk denotes a sampling point which is either the species type-locality
715 or within the type-locality area.

716 **Table S3.** Summary statistics for 61 samples included in the study. Parameters ‘proportion of
717 heterozygous sites’, ‘coverage’, and missing data’ (for Dataset II) are described in methods.
718 Samples in red did not pass the reads threshold of $\geq 500,000$ reads.

719 **Table S4.** Summary of nuclear DNA datasets generated for this study. ‘N’ represents the number
720 of individuals used in each dataset. ‘Sites’ represent the total number of nucleotides (either variable
721 or not across samples) covered in each dataset. ‘SNPs’ is an abbreviation for single-nucleotide
722 polymorphisms. Scripts used to generate the datasets are provided at [https://github.com/g-](https://github.com/g-pacheco/KryptolebiasGenomics/wiki/08.-Nuclear-Genome-Datasets)
723 [pacheco/KryptolebiasGenomics/wiki/08.-Nuclear-Genome-Datasets](https://github.com/g-pacheco/KryptolebiasGenomics/wiki/08.-Nuclear-Genome-Datasets).

724 **Figure S1.** Coqueiral beach sampling locality and *Kryptolebias* spp. specimens. (a) Freshwater
725 stream at Coqueiral beach in Aracruz, Espírito-Santo state, Brazil (19°56'3.44"S; 040° 7'48.13"W),
726 where individuals of *Kryptolebias* sp. 'ESP' and *K. hermaphroditus* 'South Clade' have been
727 collected. (b) Individual male of *K. hermaphroditus* (sensu Costa 2016) collected from the
728 sampling locality. (c) *Kryptolebias hermaphroditus* 'Southern clade' male collected in Ceará-
729 Mirim River, Extremoz, Rio Grande do Norte state, Brazil (05°40'25.88"S; 035°14'14.48"W) same
730 male as described in Berbel-Filho et al. (2016) as the first male reported for the species. (c)
731 *Kryptolebias hermaphroditus* 'South clade' (following the geographical criteria in Lira et al.
732 (2021)) male (photographed fresh after sampling) collected in mangrove forest in Viseu, Viseu,
733 Pará, Brazil (01°10'54.60"S; 46°9'31.90"W). The external differences between the previous
734 *Kryptolebias hermaphroditus* 'South clade' males (also found in Amorim et al. (2022) and the
735 ones sampled in Coqueiral beach by Costa (2016) and us (a), together with the syntopy between
736 two lineages on that sampling point our results (see Discussion) calls for further attention on the
737 taxonomic status of males as either *K. hermaphroditus* or *Kryptolebias* sp. 'ESP'.

738 **Figure S2.** Sampling sites for the 423 *Kryptolebias* individuals included in the mtDNA
739 phylogenetic reconstruction. Site details are provided in Table S1.

740 **Figure S3.** Sampling sites for the individuals included in the genetic analysis. Site names and
741 details are included in Table S2.

742 **Figure S4.** Maximum-likelihood reconstruction for 115,397 concatenated nuclear sites (Dataset I)
743 from 48 *Kryptolebias* individuals. Node values represent SH-aLRT (%), aBayes, and ultrafast
744 bootstrap (%) support values, respectively. In the tip labels, 'Kmar' (dark brown) denotes *K.*
745 *marmoratus* individuals; 'Kher_CentralClade' (light brown) represent individuals from *K.*
746 *hermaphroditus* 'Central clade'; 'Kher_SouthClade' (yellow) represent *K. hermaphroditus*

747 ‘Southern clade’ individuals; ‘KspESP’ (red) refers to *Kryptolebias* sp. ‘ESP’ individuals; ‘Koce’
748 (green) denotes *K. ocellatus* individuals; ‘Kgra’ (dark blue) denotes *K. gracilis* individuals; ‘Kbra’
749 (light blue) represents *K. brasiliensis*. Details for all samples used are provided in Table S2. All
750 species, with exception of *K. marmoratus* and *K. hermaphroditus* (represented by hermaphrodites),
751 are represented by male individuals.

752 **Figure S5.** Maximum-likelihood reconstruction for 1,631,872 concatenated nuclear sites from
753 five individuals (one representative per species) within the ‘mangrove killifish’ clade. Node values
754 represent standard bootstrap (%) support values. In the tip labels, ‘Kmar’ denotes *K. marmoratus*;
755 ‘Kher_CentralClade’ represent an individual from *K. hermaphroditus* ‘Central clade’;
756 ‘Kher_SouthClade’ represent *K. hermaphroditus* ‘Southern clade’; ‘Ksp_ESP’ refers to
757 *Kryptolebias* sp. ‘ESP’; ‘Koce’ denotes *K. ocellatus* individuals. This tree was used as our starting
758 network (hmax=0) for out phylogenetic networks analyses using PhyloNetworks v. 0.14.2 (Solís-
759 Lemus et al., 2017).

760 **Figure S6.** Phylogenetic networks reconstructed in PhyloNetworks v. 0.14.2 (Solís-Lemus et al.,
761 2017) showing reticulation events in *Kryptolebias*. Phylogenies shown here represent the tree with
762 the lowest pseudolikelihood scores for each maximum number of reticulation events (‘hmax’).
763 Blue arrow indicates the direction of reticulation, while blue numbers represent the proportion of
764 genes inherited by each parent.

765 **Figure S7.** Estimated number of genetic clusters (K) based on different metrics retrieved from
766 StructureSelector (Li and Liu, 2018). Those four metrics (median of medians (MedMedK);
767 medians of means (MedMeanK); maximum of medians (MaxMedK); maximum of the means
768 (MaxMeaK)) are implemented Puechmaille (2016) to account for unevenness of sampling sizes
769 and hierarchical structure.

770 **Figure S8.** Individual ancestry plots for each K value (2 to 8) ran in nsgAdmix with 9,532 SNPs
771 (Dataset III). Each column represents an individual and each color represents a different genetic
772 cluster.

773 **Figure legends**

774 **Figure 1.** Approximated geographic distribution of known *Kryptolebias* species and lineages.
775 Geographic distributions for the species/lineages were on the literature (Berbel-Filho et al., 2020;
776 Costa, 1990, 2004; Costa, 2007; Costa, 2006, 2016; Lira et al., 2021; Tatarenkov et al., 2017;
777 Vermeulen and Hrbek, 2005) as well as online databases for sampling records (GBIF;
778 www.gbif.org) and museum collections (CRIA - SpeciesLink; <http://splink.cria.org.br/>). Symbols
779 next to species name represent species inhabiting mangrove (mangrove tree) or freshwater (blue
780 spot) habitats.

781 **Figure 2.** Maximum-likelihood reconstruction for 49 unique *cox1* haplotypes extracted from 423
782 *Kryptolebias* individuals. (a) Full tree containing the relationships among the 49 haplotypes with
783 tip labels colored by species/lineages names. Tip labels show haplotypes and number of
784 individuals sequenced (in parenthesis). (b) Haplotype network for the 27 *cox1* haplotypes for
785 individuals belonging to the selfing mangrove killifishes clade with their respective distribution.
786 Details for all samples used for these analyses are provided in Table S1.

787 **Figure 3.** Phylogenetic reconstructions of the genus *Kryptolebias* using IQ-Tree 2 v. 2.0.1. (a)
788 Schematic representation of the maximum-likelihood phylogenetic tree based on 49 unique
789 mtDNA *cox1* haplotypes extracted from 423 *Kryptolebias* individuals. Node circles represent
790 nonparametric bootstrap values = 100. The full mtDNA phylogenetic reconstruction is provided
791 on Figure 2. (b) Maximum-likelihood phylogenetic tree based on 174,842 GBS nuclear sites
792 (Dataset I). Node circles represent SH-aLRT (%), aBayes, and ultrafast bootstrap (%) support
793 values, respectively. Only nodes with high support (SH-aLRT ≥ 90 , aBayes = 1, and ultrafast
794 bootstrap > 90) are shown. Branch lengths are shown in substitutions per site. Intraspecific clades
795 were collapsed to facilitate visualization. The full nuclear phylogenetic reconstruction is provided

796 on Supplementary Fig. S4. (c) 95% confidence phylogenetic network (Neighbor-Net) constructed
797 using SplitsTree based on all sites from Dataset II. All species, with exception of *K. marmoratus*
798 and *K. hermaphroditus* (represented by hermaphrodites), are represented in the figure by male
799 individuals.

800 **Figure 4.** Phylogenetic networks and introgression analysis in the mangrove killifishes clade.
801 Genetic structure analysis for mangrove killifish species based on 9,532 SNPs (Dataset III). (a)
802 Log-pseudolikelihood scores per number of reticulation events tested using PhyloNetworks v.
803 0.14.2 (Solís-Lemus et al., 2017). The red dot indicates the network chosen based on a large
804 improvement of the pseudolikelihood score. (b) Phylogenetic network with one reticulation event.
805 Numbers indicate inheritance proportions in the hybrid lineage. (c-e) ABBA-BABA results for
806 introgression tests between: (c) *K. hermaphroditus* ‘Central clade’ (*Kher Central*) and *K.*
807 *marmoratus* (*Kmar*); (d) *K. hermaphroditus* ‘Southern clade’ (*Kher South*) and *Kryptolebias*
808 sp. ‘ESP’ (*Ksp. ESP*); (e) *K. hermaphroditus* ‘Southern clade’ (*Kher South*) and *K. ocellatus*
809 (*Koce*).

810 **Figure 5.** Genetic structure plots for the lineages in the mangrove killifish clade. (a) Admixture
811 plot for K=5, indicated by StructureSelector (Li and Liu, 2018) as the most likely number of
812 genetic clusters based on Dataset III (9,532 SNPs). (b) Multidimensional scaling plot based on the
813 pairwise genetic distances between individuals extracted from Dataset III. (c) Proportion of
814 heterozygous sites per individual based on the site frequency spectrum for Dataset VII (863,662
815 nuclear sites). For ease of visualization, species based on data extracted from whole-genome
816 sequences (*K. marmoratus* and *K. hermaphroditus* ‘Central clade’) were omitted from the plot
817 given a very low number of heterozygous sites (see Results). All plots follow the color scheme

818 described in (b). Across all plots, individuals marked with asterisks represent *K. hermaphroditus*
819 'Southern clade' sympatric to *Kryptolebias* sp. 'ESP'.

820 **References**

- 821 Amorim, P.F., Katz, A.M., Ottoni, F.P., de Bragança, P.H.N., 2022. Genetic structure of the
822 mangrove Killifish *Kryptolebias hermaphroditus* Costa, 2011 (Cyprinodontiformes:
823 Aplocheiloidei) supports a wide connection among its populations. *Zoological Studies* 61.
- 824 Anisimova, M., Gil, M., Dufayard, J.-F., Dessimoz, C., Gascuel, O., 2011. Survey of branch
825 support methods demonstrates accuracy, power, and robustness of fast likelihood-based
826 approximation schemes. *Systematic Biology* 60, 685-699.
- 827 Avise, J., 2008. *Clonality: the genetics, ecology, and evolution of sexual abstinence in vertebrate*
828 *animals*. Oxford University Press on Demand.
- 829 Avise, J.C., Tatarenkov, A., 2015. Population genetics and evolution of the mangrove rivulus
830 *Kryptolebias marmoratus*, the world's only self-fertilizing hermaphroditic vertebrate. *J Fish*
831 *Biol* 87, 519-538.
- 832 Barrett, S.C., 2014. Evolution of mating systems: outcrossing versus selfing. *The Princeton Guide*
833 *to Evolution*, pp. 356-362.
- 834 Berbel-Filho, W.M., de Leaniz, C.G., Morán, P., Cable, J., Lima, S.M., Consuegra, S., 2019. Local
835 parasite pressures and host genotype modulate epigenetic diversity in a mixed-mating fish.
836 *Ecology and evolution* 9, 8736-8748.
- 837 Berbel-Filho, W.M., Espirito-Santo, H.M.V., Lima, S.M.Q., 2016. First record of a male of
838 *Kryptolebias hermaphroditus* Costa, 2011 (Cyprinodontiformes: Cynolebiidae). *Neotrop*
839 *Ichthyol* 14, e160024.
- 840 Berbel-Filho, W.M., Tatarenkov, A., Espirito-Santo, H.M., Lira, M.G., De Leaniz, C.G., Lima,
841 S.M., Consuegra, S., 2020. More than meets the eye: syntopic and morphologically similar

842 mangrove killifish species show different mating systems and patterns of genetic structure
843 along the Brazilian coast. *Heredity*, 1-13.

844 Berbel-Filho, W.M., Tatarenkov, A., Pacheco, G., Espírito-Santo, H., Lira, M.G., Garcia de
845 Leaniz, C., Avise, J.C., Lima, S.M., Rodríguez-López, C.M., Consuegra, S., 2021. Against
846 the odds: hybrid zones between mangrove killifish species with different mating systems.
847 *Genes* 12, 1486.

848 Bonnet, T., Leblois, R., Rousset, F., Crochet, P.A., 2017. A reassessment of explanations for
849 discordant introgressions of mitochondrial and nuclear genomes. *Evolution* 71, 2140-2158.

850 Bravo, G.A., Antonelli, A., Bacon, C.D., Bartoszek, K., Blom, M.P., Huynh, S., Jones, G.,
851 Knowles, L.L., Lamichhaney, S., Marcussen, T., 2019. Embracing heterogeneity: coalescing
852 the Tree of Life and the future of phylogenomics. *PeerJ* 7, e6399.

853 Browning, B.L., Tian, X., Zhou, Y., Browning, S.R., 2021. Fast two-stage phasing of large-scale
854 sequence data. *The American Journal of Human Genetics* 108, 1880-1890.

855 Brys, R., Van Cauwenberghe, J., Jacquemyn, H., 2016. The importance of autonomous selfing in
856 preventing hybridization in three closely related plant species. *Journal of Ecology* 104, 601-
857 610.

858 Bushnell, B., 2014. BBMap: a fast, accurate, splice-aware aligner. Lawrence Berkeley National
859 Lab.(LBNL), Berkeley, CA (United States).

860 Choi, B.-S., Park, J.C., Kim, M.-S., Han, J., Kim, D.-H., Hagiwara, A., Sakakura, Y., Hwang, U.-
861 K., Lee, B.-Y., Lee, J.-S., 2020. The reference genome of the selfing fish *Kryptolebias*
862 *hermaphroditus*: Identification of phases I and II detoxification genes. *Comparative*
863 *Biochemistry and Physiology Part D: Genomics and Proteomics* 35, 100684.

864 Costa, W., 1990. Description d'une nouvelle espèce du genre *Rivulus* (Cyprinodontiformes,
865 Rivulidae) de l'Amazone orientale. *Revue française d'aquariologie herpétologie* 17, 41-44.

866 Costa, W., 2004. Relationships and redescription of *Fundulus brasiliensis* (Cyprinodontiformes:
867 Rivulidae), with description of a new genus and notes on the classification of the
868 Aplocheiloidei. *Ichthyol Explor Fres* 15, 105-120.

869 Costa, W., 2009. Peixes aplocheilóideos da Mata Atlântica brasileira: história, diversidade e
870 conservação/Aplocheiloid fishes of the Brazilian Atlantic Forest: history, diversity and
871 conservation. Rio de Janeiro: Museu Nacional UFRJ, 172.

872 Costa, W.J., 2007. *Kryptolebias gracilis* n. sp.(Teleostei: Cyprinodontiformes: Rivulidae): a new
873 killifish from the Saquarema Lagoon basin, southeastern Brazil. *aqua* 13, 7.

874 Costa, W.J.E.M., 2006. Redescription of *Kryptolebias ocellatus* (Hensel) and *K. caudomarginatus*
875 (Seegers)(Teleostei: Cyprinodontiformes: Rivulidae), two killifishes from mangroves of
876 south-eastern Brazil. *Aqua: Journal of Ichthyology & Aquatic Biology* 11, 5-13.

877 Costa, W.J.E.M., 2011a. Identity of *Rivulus ocellatus* and a new name for a hermaphroditic species
878 of *Kryptolebias* from south-eastern Brazil (Cyprinodontiformes: Rivulidae). *Ichthyol Explor*
879 *Fres* 22, 185-192.

880 Costa, W.J.E.M., 2011b. Phylogenetic position and taxonomic status of *Anablepsoides*,
881 *Atlantirivulus*, *Cynodonichthys*, *Laimosemion* and *Melanorivulus* (Cyprinodontiformes:
882 Rivulidae). *Ichthyol Explor Fres* 22, 233-249.

883 Costa, W.J.E.M., 2016. Colouration, taxonomy and geographical distribution of mangrove
884 killifishes, the *Kryptolebias marmoratus* species group, in southern Atlantic coastal plains of
885 Brazil (Cyprinodontiformes: Rivulidae). *Ichthyol Explor Fres* 27, 183-192.

886 Costa, W.J.E.M., Lima, S.M.Q., Bartolette, R., 2010. Androdioecy in *Kryptolebias* killifish and
887 the evolution of self-fertilizing hermaphroditism. *Biol J Linn Soc* 99, 344-349.

888 Clement, M., Snell, Q., Walker, P., Posada, D., Crandall, K. 2002. TCS: Estimating gene
889 genealogies. *Parallel and Distributed Processing Symposium, International Proceedings*, 2,
890 184.

891 Eriksson, A. and Manica, A., 2012. Effect of ancient population structure on the degree of
892 polymorphism shared between modern human populations and ancient hominins. *Proceedings*
893 *of the National Academy of Sciences*, 109,13956-13960.

894 Furness, A.I., Tatarenkov, A., Avise, J.C., 2015. A genetic test for whether pairs of hermaphrodites
895 can cross-fertilize in a selfing killifish. *Journal of Heredity* 106, 749-752.

896 Guimarães-Costa, A., Schneider, H., Sampaio, I., 2017. New record of the mangrove rivulid
897 *Kryptolebias hermaphroditus* Costa, 2011 (Cyprinodontiformes: Cynolebiidae) in the Pará
898 state, northern Brazil. *Check List* 13, 2093.

899 Guindon, S., Dufayard, J.-F., Lefort, V., Anisimova, M., Hordijk, W., Gascuel, O., 2010. New
900 algorithms and methods to estimate maximum-likelihood phylogenies: assessing the
901 performance of PhyML 3.0. *Systematic biology* 59, 307-321.

902 Hahn, M.W., Nakhleh, L., 2016. Irrational exuberance for resolved species trees. *Evolution* 70, 7-
903 17.

904 Hatem, A., Bozdağ, D., Toland, A.E., Çatalyürek, Ü.V., 2013. Benchmarking short sequence
905 mapping tools. *BMC Bioinformatics* 14, 184.. doi:10.1186/1471-2105-14-184.

906 Harrington, R.W., 1971. How ecological and genetic factors interact to determine when self-
907 fertilizing hermaphrodites of *Rivulus marmoratus* change into functional secondary males,
908 with a reappraisal of the modes of intersexuality among fishes. *Copeia*, 389-432.

909 Herten, K., Hestand, M.S., Vermeesch, J.R., Van Houdt, J.K., 2015. GBSX: a toolkit for
910 experimental design and demultiplexing genotyping by sequencing experiments. BMC
911 Bioinformatics 16, 73.

912 Hibbins, M.S., Hahn, M.W., 2022. Phylogenomic approaches to detecting and characterizing
913 introgression. Genetics 220.

914 Hoang, D.T., Chernomor, O., Von Haeseler, A., Minh, B.Q., Vinh, L.S., 2018. UFBoot2:
915 improving the ultrafast bootstrap approximation. Molecular Biology and Evolution 35, 518-
916 522.

917 Huson, D.H., Bryant, D., 2006. Application of phylogenetic networks in evolutionary studies.
918 Molecular Biology and Evolution 23, 254-267.

919 Jeffroy, O., Brinkmann, H., Delsuc, F., Philippe, H., 2006. Phylogenomics: the beginning of
920 incongruence? Trends in Genetics 22, 225-231.

921 Kalyaanamoorthy, S., Minh, B.Q., Wong, T.K., Von Haeseler, A., Jermini, L.S., 2017.
922 ModelFinder: fast model selection for accurate phylogenetic estimates. Nature Methods 14,
923 587-589.

924 Kanamori, A., Sugita, Y., Yuasa, Y., Suzuki, T., Kawamura, K., Uno, Y., Kamimura, K., Matsuda,
925 Y., Wilson, C.A., Amores, A., Postlethwait, J.H., Suga, K., Sakakura, Y., 2016. A genetic
926 map for the only self-fertilizing vertebrate. G3: Genes, Genomes, Genetics 6, 1095-1106.

927 Kitimu, S.R., Taylor, J., March, T.J., Tairo, F., Wilkinson, M.J., Rodríguez López, C.M., 2015.
928 Meristem micropropagation of cassava (*Manihot esculenta*) evokes genome-wide changes in
929 DNA methylation. Frontiers in Plant Science 6, 590.

930 Korneliussen, T.S., Albrechtsen, A., Nielsen, R., 2014. ANGSD: analysis of next generation
931 sequencing data. BMC Bioinformatics 15, 356.

932 Langmead, B., Salzberg, S.L., 2012. Fast gapped-read alignment with Bowtie 2. *Nature Methods*
933 9, 357-359.

934 Li, H., Durbin, R., 2009. Fast and accurate short read alignment with Burrows-Wheeler transform.
935 *Bioinformatics* 25, 1754–1760.. doi:10.1093/bioinformatics/btp324

936 Li, H., Handsaker, B., Wysoker, A., Fennell, T., Ruan, J., Homer, N., Marth, G., Abecasis, G.,
937 Durbin, R., Genome Project Data Processing, S., 2009. The sequence alignment/map format
938 and SAMtools. *Bioinformatics* 25, 2078-2079.

939 Li, Y.L., Liu, J.X., 2018. StructureSelector: A web-based software to select and visualize the
940 optimal number of clusters using multiple methods. *Mol Ecol Resour* 18, 176-177.

941 Lins, L.S.F., Trojahn, S., Sockell, A., Yee, M.C., Tatarenkov, A., Bustamante, C.D., Earley, R.L.,
942 Kelley, J.L., 2018. Whole-genome sequencing reveals the extent of heterozygosity in a
943 preferentially self-fertilizing hermaphroditic vertebrate. *Genome* 61, 241-247.

944 Lira, M.G., Berbel-Filho, W.M., Espírito-Santo, H.M., Tatarenkov, A., Avise, J.C., Garcia de
945 Leaniz, C., Consuegra, S., Lima, S.M., 2021. Filling the gaps: phylogeography of the self-
946 fertilizing *Kryptolebias* species (Cyprinodontiformes: Rivulidae) along South American
947 mangroves. *J Fish Biol*, 644-655.

948 Lomax, J.L., Carlson, R.E., Wells, J.W., Crawford, P.M., Earley, R.L., 2017. Factors affecting egg
949 production in the selfing mangrove rivulus (*Kryptolebias marmoratus*). *Zoology* 122, 38-45.

950 Maddison, W.P., 1997. Gene trees in species trees. *Systematic Biology* 46, 523-536.

951 Malinsky, M., Matschiner, M., Svardal, H., 2021. Dsuite-Fast D-statistics and related admixture
952 evidence from VCF files. *Mol Ecol Resour* 21, 584-595.

953 Mallet, J., 2005. Hybridization as an invasion of the genome. *Trends in Ecology & Evolution* 20,
954 229-237.

955 Mallet, J., Besansky, N., Hahn, M.W., 2016. How reticulated are species? *Bioessays* 38, 140-149.

956 Minh, B.Q., Schmidt, H.A., Chernomor, O., Schrempf, D., Woodhams, M.D., Von Haeseler, A.,
957 Lanfear, R., 2020. IQ-TREE 2: new models and efficient methods for phylogenetic inference
958 in the genomic era. *Molecular Biology and Evolution* 37, 1530-1534.

959 Murphy, W.J., Thomerson, J.E., Collier, G.E., 1999. Phylogeny of the Neotropical killifish family
960 Rivulidae (Cyprinodontiformes, Aplocheiloidei) inferred from mitochondrial DNA
961 sequences. *Mol Phylogenet Evol* 13, 289-301.

962 Nakhleh, L., 2013. Computational approaches to species phylogeny inference and gene tree
963 reconciliation. *Trends in Ecology & Evolution* 28, 719-728.

964 Olave, M., Meyer, A., 2020. Implementing large genomic single nucleotide polymorphism data
965 sets in phylogenetic network reconstructions: a case study of particularly rapid radiations of
966 cichlid fish. *Systematic Biology* 69, 848-862.

967 Pickup, M., Brandvain, Y., Fraïsse, C., Yakimowski, S., Barton, N.H., Dixit, T., Lexer, C.,
968 Cereghetti, E., Field, D.L., 2019. Mating system variation in hybrid zones: facilitation,
969 barriers and asymmetries to gene flow. *New Phytol* 224, 1035-1047.

970 Sarmiento-Soares, L.M., Ingenito, L.F., Duboc, L., Martins-Pinheiro, R., Borçato, R., Silva, J.,
971 2014. Primeiros registros de *Kryptolebias ocellatus* (Hensel)(Cyprinodontiformes, Rivulidae)
972 para riachos de Mata Atlântica no Espírito Santo. *Boletim Sociedade Brasileira de Ictiologia*
973 111, 15-19.

974 Schubert, M., Ermini, L., Der Sarkissian, C., Jónsson, H., Ginolhac, A., Schaefer, R., Martin,
975 M.D., Fernández, R., Kircher, M., McCue, M., 2014. Characterization of ancient and modern
976 genomes by SNP detection and phylogenomic and metagenomic analysis using PALEOMIX.
977 *Nature Protocols* 9, 1056-1082.

978 Schubert, M., Lindgreen, S., Orlando, L., 2016. AdapterRemoval v2: rapid adapter trimming,
979 identification, and read merging. BMC Research Notes 9.. doi:10.1186/s13104-016-1900-2

980 Skotte, L., Korneliussen, T.S., Albrechtsen, A., 2013. Estimating individual admixture proportions
981 from next generation sequencing data. Genetics 195, 693-702.

982 Solís-Lemus, C., Bastide, P., Ané, C., 2017. PhyloNetworks: a package for phylogenetic networks.
983 Molecular Biology and Evolution 34, 3292-3298.

984 Tatarenkov, A., Earley, R.L., Taylor, D.S., Davis, W.P., Avise, J.C., 2018. Natural hybridization
985 between divergent lineages in a selfing hermaphroditic fish. Biol Letters 14, 20180118.

986 Tatarenkov, A., Earley, R.L., Taylor, D.S., Davis, W.P., Avise, J.C., 2021. Extensive hybridization
987 and past introgression between divergent lineages in a quasi-clonal hermaphroditic fish:
988 ramifications for species concepts and taxonomy. J Evolution Biol 34, 49-59.

989 Tatarenkov, A., Lima, S.M.Q., Avise, J.C., 2011. Extreme homogeneity and low genetic diversity
990 in *Kryptolebias ocellatus* from south-eastern Brazil suggest a recent foundation for this
991 androdioecious fish population. J Fish Biol 79, 2095-2105.

992 Tatarenkov, A., Lima, S.M.Q., Earley, R.L., Berbel-Filho, W.M., Vermeulen, F.B.M., Taylor,
993 D.S., Marson, K., Turner, B.J., Avise, J.C., 2017. Deep and concordant subdivisions in the
994 self-fertilizing mangrove killifishes (*Kryptolebias*) revealed by nuclear and mtDNA markers.
995 Biological Journal of the Linnean Society 122, 558-578.

996 Tatarenkov, A., Lima, S.M.Q., Taylor, D.S., Avise, J.C., 2009. Long-term retention of self-
997 fertilization in a fish clade. Proceedings of the National Academy of Sciences 106, 14456-
998 14459.

999 Taylor, S.A., Larson, E.L., 2019. Insights from genomes into the evolutionary importance and
1000 prevalence of hybridization in nature. Nature Ecology and Evolution 3, 170-177.

1001 Thompson, A.W., Wojtas, H., Davoll, M., Braasch, I., 2022. Genome of the Rio Pearlfish
1002 (Nematolebias whitei), a bi-annual killifish model for Eco-Evo-Devo in extreme
1003 environments. G3 Genes|Genomes|Genetics.

1004 Toews, D.P., Brelsford, A., 2012. The biogeography of mitochondrial and nuclear discordance in
1005 animals. Molecular Ecology 21, 3907-3930.

1006 Vermeulen, F.B., Hrbek, T., 2005. *Kryptolebias sepia* n. sp. (Actinopterygii: Cyprinodontiformes:
1007 Rivulidae), a new killifish from the Tapanahony River drainage in southeast Surinam.
1008 Zootaxa 928, 1-20.

1009 Vieira, F.G., Lassalle, F., Korneliussen, T.S., Fumagalli, M., 2015. Improving the estimation of
1010 genetic distances from Next-Generation sequencing data. Biol J Linn Soc 117, 139-149.

1011 Weibel, A.C., Dowling, T.E., Turner, B.J., 1999. Evidence that an outcrossing population is a
1012 derived lineage in a hermaphroditic fish (*Rivulus marmoratus*). Evolution 53, 1217-1225.

1013